

# Remote Sensing of Land Change: A Multifaceted Perspective

1 **Zhe Zhu\*** and Shi Qiu

2 Department of Natural Resources and the Environment, University of Connecticut, Storrs, CT, USA

3 **\* Correspondence:**

4 zhe@uconn.edu

5 **Keywords:** land change, remote sensing, multifaceted, land cover change, land disturbance, climate  
6 variability, climate change, succession, time series.

7 **Abstract**

8 The discipline of land change science has been evolving rapidly in the past decades. Remote sensing  
9 played a major role in one of the most critical components of land change science, which includes  
10 observation, monitoring, and characterization of land change. In this paper, we proposed a new  
11 framework of the multifaceted view of land change through the lens of remote sensing and  
12 recommended five facets of land change including change location, time, target, process, and agent.  
13 We also evaluated the impact of spatial, spectral, temporal, and angular dimensions of the remotely  
14 sensed data on observing, monitoring, and characterization of different facets of land change, as well  
15 as discussed some of the current land change products. We recommend clarifying the specific land  
16 change facet being studied in all remote sensing of land change efforts, reporting multiple or full  
17 facets of land change in remote sensing products, shifting the focus from land cover change to  
18 identify the specific change process and agent, integrating socioeconomic data as well as new social-  
19 environment framework for a deeper and fuller understanding of land change, and recognizing the  
20 limitations and weaknesses of remote sensing platforms in land change studies.

## 21 **1 Introduction**

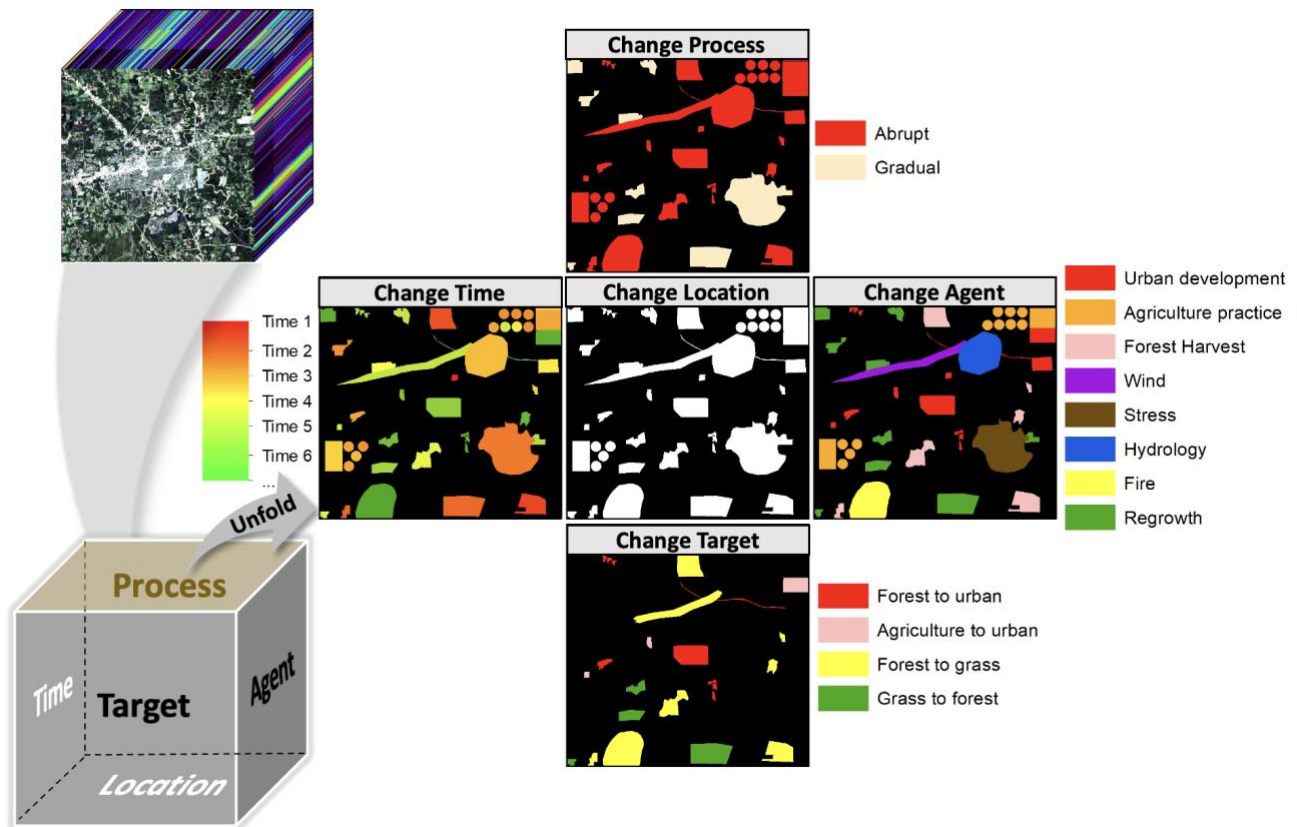
22 With the increasing contemporary concerns on climate change, global environmental change, and  
23 sustainability, land change science emerged as a unique science direction for addressing these knotty  
24 issues (Gutman et al., 2004; Rindfuss et al., 2004; Turner et al., 2007). Land change science, defined  
25 as “the interdisciplinary field seeks to understand the dynamics of land cover and land use as a  
26 coupled human-environment system to address theory, concepts, models, and applications relevant to  
27 environmental and societal problems, including the intersection of the two” (Turner et al., 2007), has  
28 many components, in which one of the most fundamental and critical components is the observation,  
29 monitoring, and characterization of land change.

30  
31 The terrestrial surface of the Earth has been modified or transformed by humans at an unprecedented  
32 rate. More than half of the Earth’s ice-free land surface has been affected by humans (Ellis et al.,  
33 2010), and almost all land surfaces have been influenced by climate change and various kinds of land  
34 disturbances (Dale, 1997; Potter et al., 2003). Remote sensing, particularly satellite remote sensing,  
35 that can provide synoptic and repeated measurements of the global land surface at different spectral,  
36 spatial, and temporal resolutions are of great importance for studying global land change (Justice et  
37 al., 1998; Roy et al., 2014; Sellers et al., 1995). In the past decades, big advancements have been  
38 made in large-scale mapping of land change based on remote sensing data, due to the rapidly growing  
39 amounts of earth observation satellites (Belward and Skøien, 2015; Ustin and Middleton, 2021), the  
40 free and open data policy (Woodcock et al., 2008; Wulder et al., 2012; Zhu et al., 2019), the analysis-  
41 ready data format (Dwyer et al., 2018; Frantz, 2019; Zhu, 2019), the increasing computing  
42 capabilities (Gorelick et al., 2017; Ma et al., 2015), and the availability of new algorithms for change  
43 detection (Banskota et al., 2014; Kennedy et al., 2014; Zhu, 2017). Recently, a paradigm shift from  
44 change detection of two points in time to monitoring and tracking change continuously in time is  
45 observed in remote sensing community, where the use of dense time-series observations is more

46 common and new land change information, such as subtle changes in ecosystem health and condition  
47 and long-term trend of the vegetation productivity, is more reachable (Woodcock et al., 2020).  
48 Moreover, land change information can now be monitored in near real-time (Verbesselt et al., 2012;  
49 Xin et al., 2013; Ye et al., 2021a), which greatly improves its value to resource managers and  
50 policymakers. We have also witnessed a proliferation of land change characterization algorithms  
51 (Zhu, 2017), with majority of them focusing on the “from-to” information, that is, land cover and/or  
52 land use information before and after the change (Hansen and Loveland, 2012; Pricope et al., 2019).  
53 It should be noted that though land cover (the physical properties at the Earth’s surface) and land use  
54 (the social, economic, and cultural utility of land) are quite distinct (Turner, 1997), they are often  
55 grouped together in remote sensing products, and land cover is usually used as a surrogate for  
56 understanding land use, such as including cropland and developed in the categories of land cover  
57 (Anderson et al., 1976). Considering remote sensing data provide information on land cover, rather  
58 than on land use, we will mainly focus on land cover change here.

59  
60 In this paper, we propose the framework of multifaceted perspective in remote sensing of land  
61 change, in which the change in land cover is only one of the components viewed from one of the five  
62 facets of land change -- the target of change or what is changing (Fig. 1). Basically, if we detect  
63 change in satellite spectral bands, we can extract land change information to answer five different  
64 questions, that are, when (change time), where (change location), what (change target), how (change  
65 process), and why (change agent) the change happened. Each of the questions will occupy one facet  
66 of the change cube that contains the spectral change information derived from remotely sensed data.  
67 The facet on the top of the change cube is left empty on purpose (Fig. 1), as there may be other facets  
68 of land change that are not discussed here. The two facets on “Time” and “Location” provide  
69 information on observation and monitoring of land change, and the other three facets on “Target”,  
70 “Process”, and “Agent” are related to the characterization of land change. In this paper, we will first

71 discuss all five facets of land change as well as their relationship through the lens of remote sensing.  
 72 Next, we will discuss the remote sensing issues in spectral, spatial, temporal, and angular domains in  
 73 observing, monitoring, and characterization of different facets of land change. Finally, we will  
 74 discuss some of the current land change products derived from remote sensing data and conclude  
 75 with future recommendations.  
 76

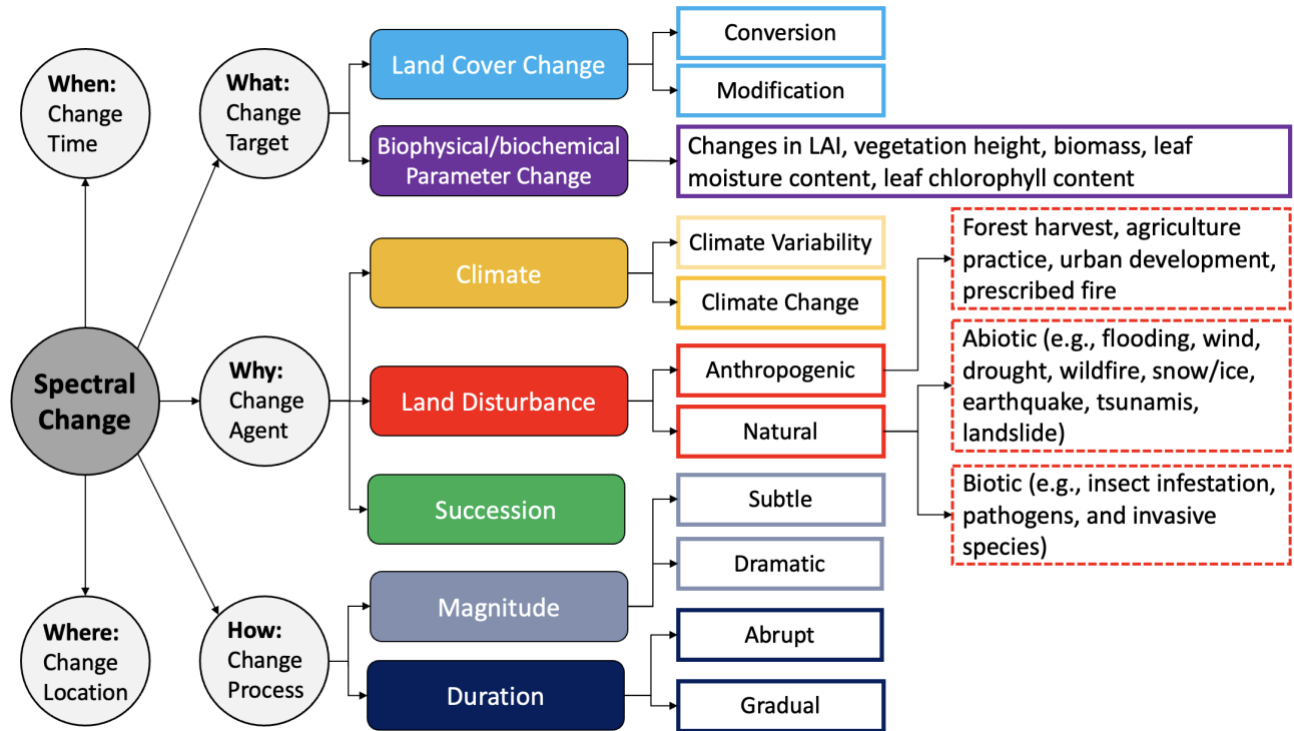


77  
 78 **Fig. 1.** The five facets proposed for observation, monitoring, and characterization of land change  
 79 using remotely sensed data. It is worth noting that not all land change agent will lead to a change in  
 80 change target or land cover in this case, and some of the change patches shown in the other four  
 81 facets are not shown (e.g., stress, hydrology, agriculture practice) or only partially shown (e.g., wind,  
 82 urban development, and regrowth) in the facet of land change target.  
 83

84 **2 The five facets of land change**

85 If the remote sensing system is well designed for capturing the specific land change type, it is  
 86 possible to extract land change information for five different facets based on the remotely sensed  
 87 observations collected before, during, and/or after the land change (Fig. 2).

88



89  
 90  
 91

**Fig. 2.** Hierarchical classification system for the five facets of land change.

## 92 2.1 Where - Change Location

93 The first facet of land change is to answer the question of where the change has occurred or  
 94 determine the change location. Theoretically, by differencing two georeferenced remotely sensed  
 95 images collected at a different time from the same spectral band and same location, any kind of land  
 96 surface change that occurred between the two dates would have larger difference values than places  
 97 that have not changed. By using a simple threshold, the location of change could be identified easily.  
 98 The land change detected in this way is sometimes called “spectral change”, as clearly there is a  
 99 spectral value change between the two dates of the remotely sensed images, but this does not always  
 100 correspond to the changes on the land surface. Other factors, such as image registration, atmospheric

101 condition, natural soil wetness fluctuation, vegetation phenology, sensor-solar-geometry, topography  
102 illumination, will all contribute to the spectral change (Kennedy et al., 2014; Zhu, 2017). Therefore,  
103 one of the most critical steps before the remotely sensed images are used for detecting land change is  
104 removing or at least reducing changes in spectral values that are not caused by land surface change.  
105 Advanced algorithms have been developed to provide more accurate image registration results (Gao  
106 et al., 2009; Yan et al., 2016), perform atmospheric correction and cloud/cloud shadow detection  
107 (Masek et al., 2006; Qiu et al., 2019b; Zhu and Woodcock, 2012), include precipitation information  
108 (Tollerud et al., 2020), model and exclude seasonality (mostly driven by phenology) (Verbesselt et  
109 al., 2010; Zhu et al., 2020; Zhu and Woodcock, 2014), apply Bidirectional Reflectance Distribution  
110 Function (BRDF) to correct sensor-solar-geometry (Roy et al., 2016; Schaaf et al., 2002), remove  
111 bandpass difference (Claverie et al., 2018; Shang and Zhu, 2019), and perform topographic  
112 corrections (Buchner et al., 2020; Tan et al., 2013). It is worth noting that though these algorithms  
113 have the potential to reduce spectral changes that are not related to changes on land surface, they may  
114 also introduce artifacts, and it is not always necessary to apply all these algorithms before conducting  
115 change detection (Qiu et al., 2019a; Song et al., 2001).

## 116 **2.2 When - Change Time**

117 The second facet of land change is to answer the question of when the change occurred or determine  
118 the change time. Basically, the closer the two images are selected for detecting change, the more  
119 accurate the change time can be determined. Compared to detecting change based on real images,  
120 there are also new change detection methods that difference the model predicted values with actual  
121 remote sensing observations to identify land change (Verbesselt et al., 2012; Zhu and Woodcock,  
122 2014) and the detected change time is determined based on how soon the new clear observations are  
123 collected for each pixel location. These time-series based approaches do not need to wait for two  
124 clear remote sensing images and can provide more rapid change detection results. The remote sensing

125 community has shifted from using images collected from decades apart, to annual, and is currently  
126 shifting all the way to near-real-time change detection (Tang et al., 2019; Verbesselt et al., 2012;  
127 Woodcock et al., 2020; Ye et al., 2021a). This is particularly true with the successful launch of  
128 Sentinel-2 A/B (Drusch et al., 2012), Landsat 9 (Masek et al., 2020), and the hundreds of orbiting  
129 CubeSats (Huang and Roy, 2021) that could provide subweekly or even daily land surface  
130 observations at medium to high spatial resolutions (Li and Roy, 2017; Roy et al., 2021).

### 131 **2.3 What - Change Target**

132 The third and probably the most studied facet of land change is to answer the question of what is  
133 changing or determine the change target. The change target is sometimes defined as changes in  
134 categorical classes such as land cover type (e.g., *forest, urban, water, grass, shrub, snow/ice,*  
135 *agriculture*, etc.), or defined as changes in continuous variables of biophysical/biochemical  
136 parameters, such as Impervious Surface Area (ISA), land surface temperature, Leaf Area Index  
137 (LAI), vegetation height, biomass, leaf moisture content, leaf chlorophyll content, etc. Remotely  
138 sensed data contains rich information on the characteristics of the land surface. Feature space of more  
139 than a few dozens to even hundreds of dimensions could be created from the electromagnetic  
140 radiation (EMR) that is recorded at different wavelengths, the texture of the spectral bands, and the  
141 intra-annual/inter-annual temporal trajectory from the time series observations, to determine the land  
142 cover based on image classification (Gómez et al., 2016) or to estimate the biophysical/biochemical  
143 parameters based on machine learning or regression from empirical models (Garbulsky et al., 2011;  
144 Lin et al., 2020; Verrelst et al., 2015).

145

146 Theoretically, if we can create land cover or biophysical/biochemical parameter maps accurately at  
147 different time points, we can compare their maps to identify changes in different land cover or a  
148 specific biophysical/biochemical parameter. However, as land changes are usually very small in size

149 (e.g., 1-5% of the land surface) (Hansen et al., 2013; Song et al., 2018), and all image classification  
150 and biophysical/biochemical parameter retrieval algorithms contain errors, comparing maps of land  
151 cover or biophysical/biochemical parameters at different time points to detect land change will lead  
152 to compounded errors in the final change map at a magnitude way larger than the total change area  
153 (Olofsson et al., 2013). For example, if we assume the classification error is randomly distributed and  
154 the overall accuracy is 90%, the compounded error of change map by differencing the two land cover  
155 maps is  $100\% - 90\% \times 90\% = 19\%$  of the image, which is approximately four times of the land  
156 change area (if it is 5% of the total area). Therefore, land change is usually detected based on the  
157 magnitude of spectral change, and if a spectral change is detected, we can then estimate land cover or  
158 biophysical/biochemical parameters before and after the spectral change (Deng and Zhu, 2020; Jin et  
159 al., 2019; Zhu and Woodcock, 2014). It is worth noting that even if there is a spectral change  
160 detected, the classified categorical land cover type may still be the same, as the land change that  
161 occurred on this land cover may not be dramatic enough to change the land cover types, and we  
162 usually call this land cover modification or land cover condition change. For example, if forest cover  
163 is defined as trees covering more than 10% of the pixel following the U.S. Forest Service definition  
164 (Riemann et al., 2010), and if selective logging is reducing forest cover from 90% to 30%, we are  
165 very likely to detect a spectral change, but based on the definition, the land cover is still forest before  
166 and after the spectral change. However, if the forest harvest is reducing forest cover from 90% to 5%,  
167 then the land cover will be likely changed from forest to barren or grass, and we usually call this land  
168 cover conversion, which are corresponding to more substantial land changes that cause land cover  
169 transitions from one to another. In the remote sensing community, huge efforts have been given to  
170 land cover conversions, but fewer studies have addressed the land cover modification issues, which  
171 may be at a scale similar to or even larger than land cover conversion (Asner et al., 2005; Qin et al.,  
172 2021). Detecting land cover modification is inherently difficult in remote sensing, as the subtle  
173 spectral change signal may be at a change magnitude similar to other background noise. Subpixel

174 analyzing methods, such as spectral mixture analysis (Asner et al., 2009), continuous fields (Hansen  
175 and DeFries, 2004), fuzzy (or soft) classification (Foody and Doan, 2007), and the continuous  
176 subpixel monitoring approach (Deng and Zhu, 2020), have shown their capability in detection of land  
177 cover modification at subpixel scales.

## 178 **2.4 How - Change Process**

179 The fourth facet of land change is to answer the question of how it is changing or determine the  
180 change process (Kennedy et al., 2014; Petit et al., 2001). As remotely sensed data measure land  
181 surface reflected or emitted EMR, changes occurred on the land surface will also likely cause  
182 changes in the spectral band at the corresponding time, making remote sensing data particularly  
183 useful for tracking the land surface change trajectories and studying the specific change process  
184 (Kennedy et al., 2014). The most important remote sensing observations for studying change process  
185 are the ones that are collected during the land change events, and we can describe the change process  
186 based on the duration and magnitude of land change.

187

188 According to the change duration, change process can be divided into abrupt change and gradual  
189 change. Most of the remote sensing change detection algorithms are developed to detect abrupt  
190 changes that occur within a short time in response to a punctuated event, as these changes can be  
191 detected directly by comparing two remotely sensed images collected at different time points before  
192 and after the change event (Coppin and Bauer, 1996; Woodcock et al., 2020). On the hand other,  
193 gradual changes usually last for a much longer time as a result from a variety of causes such as  
194 damage to vegetation from disease and insects, ecological succession, and climate change  
195 (Vogelmann et al., 2016, 2012). There are also remote sensing methods developed to quantify  
196 gradual changes based on long-term time series observations (e.g., > 10 years), and algorithms that  
197 could address gradual and abrupt changes simultaneously are appearing and could provide more

198 accurate estimation of gradual changes (De Jong et al., 2012; Vogelmann et al., 2016; Zhe Zhu et al.,  
199 2016).

200

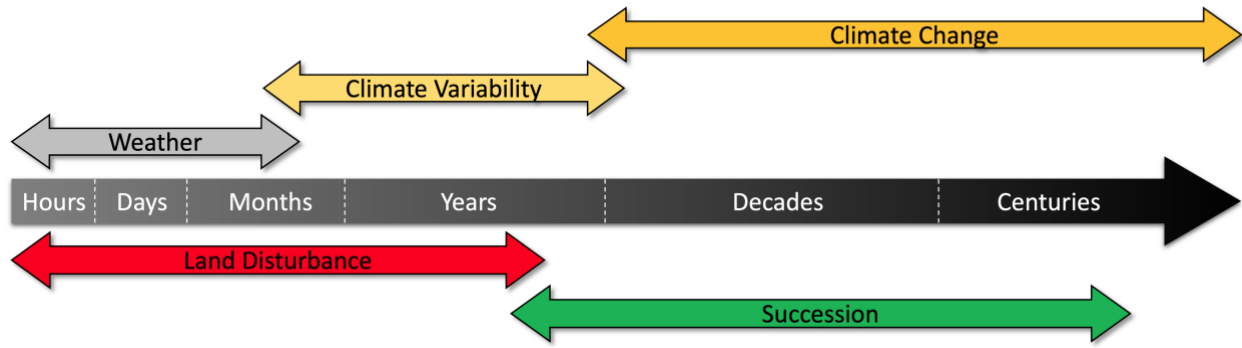
201 Based on the change magnitude, change process can be divided into subtle change and dramatic  
202 change. Subtle change modifies the land cover and the impact could be either ephemeral in time,  
203 which is sometimes called ephemeral change (e.g., gypsy moth infestation and flooding) or persistent  
204 at a much longer time (e.g., > 1 year), which is also called gradual change. Dramatic change is  
205 mainly caused by severe disturbance events, which usually lead to land cover conversion. Dramatic  
206 change is relatively easy to identify as large differences will be observed in remotely sensed imagery,  
207 but subtle change detection is much more difficult and requires change agent- or land cover-specific  
208 algorithms that are carefully calibrated against the kind of subtle change to be identified (Ye et al.,  
209 2021b). It is worth noting that other variables could also provide information on the temporal  
210 trajectories of land change for studying change process, such as time since last change, spectral  
211 stability period, and occurrence change intensity (Brown et al., 2020; Pekel et al., 2016).

212

## 213 **2.5 Why - Change Agent**

214 The fifth facet of land change is to answer the question of why it is changing or determine the change  
215 agent. Climate, land disturbance, and succession are the three major change agents that occur at quite  
216 different timescales (Fig. 3). Though the three change agents are quite different conceptually, they  
217 actually interplay with various kinds of positive and negative feedbacks (Dale et al., 2001; Guo et al.,  
218 2018; Johnson and Miyanishi, 2021; Laflouer et al., 2016; Seidl et al., 2017).

219



220

221 **Fig. 3.** Timescales applicable to weather, climate variability, climate change, land disturbance, and  
 222 succession.

223

224 Land disturbance has been defined in various ways (Clements, 1916; Grime, 1977; Sousa, 1984;

225 Turner, 2010; White and Pickett, 1985), and one of the most commonly used definitions by

226 ecologists is “any relatively discrete event in time that disrupts ecosystems, community or population

227 structure and changes resources, substrate availability, or the physical environment” (White and

228 Pickett, 1985). Zhu et al. (2020) modified and simplified this definition for detecting land disturbance

229 based on satellite time series, in which land disturbance is defined as “any discrete event that occurs

230 outside the range of natural variability of land surface”. Most of the time, land disturbance occurs in a

231 very short time ranging from hours to years and can be anthropogenic or natural. Anthropogenic

232 disturbance, sometimes called mechanical change or land use change, refers to human activity-related

233 land change, such as *forest harvest, agriculture practice, urban development, and prescribed fire.*

234 Natural disturbance can be further divided into abiotic disturbance, such as *wildfire, flooding, wind,*

235 *drought, snow/ice, earthquake, tsunamis, landslide,* and biotic disturbance, such as *insect infestation,*

236 *pathogens, and invasive species.* It is worth noting that there is a long debate on whether drought

237 should be included as one type of land disturbance, and it has only started to be considered as a

238 disturbance over the past decade (Peters et al., 2011). Fire can be both natural (wildfires) and

239 anthropogenic (prescribed fires) (Bowman et al., 2011), and remote sensing can detect both burning

240 fires and fire burned areas (Justice et al., 2002; Lentile et al., 2006). Most remote sensing algorithms  
241 developed for detecting disturbance are only limited to a single change target, such as forest  
242 disturbance (Healey et al., 2018; Huang et al., 2010; Jin and Sader, 2005; Kennedy et al., 2007; Zhu  
243 et al., 2012), and only a few algorithms can provide more general disturbance results, such as the  
244 MODIS Global Disturbance Index (MGDI) algorithm (Mildrexler et al., 2009), the LandTrendr  
245 Landsat time-series-based algorithms (Kennedy et al., 2015), and the COntinuous monitoring of  
246 Land Disturbance (COLD) algorithm (Zhu et al., 2020). As disturbance will create a spectral change  
247 signal that is outside the range of natural variability of land surface, it can be captured after the range  
248 of natural variability is well defined. However, for certain disturbance types, such as selective  
249 logging and insect infestation, they may only change a small fraction of the pixel or slightly change  
250 the health condition of the ecosystem, which makes these kinds of disturbance agents extremely hard  
251 to detect and distinguish in remote sensing data (Asner et al., 2005; Senf et al., 2017; Ye et al.,  
252 2021b).

253  
254 Unlike weather that describes current atmospheric condition (e.g., rainstorms and tropical cyclones)  
255 that changes every hour, day, and maybe months, climate measures the mean and variability of  
256 temperature, precipitation, or wind for a much longer time, ranging from months to centuries, in  
257 which climate variability refers to the short-term (e.g., months, seasons, or years) variation in climate  
258 patterns such as El-Niño Southern Oscillation, and climate change refers to the long-term changes  
259 (e.g., decades or centuries) in climates such as global warming and sea-level rise. Climate variability  
260 can be detected using remotely sensed vegetation indices by comparing a certain year with a baseline  
261 computed from a longer satellite time series (Saleska et al., 2007; Samanta et al., 2010), and climate  
262 change can be also evaluated based on the long-term trend of remotely sensed vegetation indices  
263 (Myneni et al., 1997; Zaichun Zhu et al., 2016). As both climate variability and disturbance will  
264 cause remote sensing observations to deviate abruptly from past trajectories with a spectral change

265 magnitude larger than the natural variability, climate variability is sometimes identified as one kind  
266 of disturbance type in remote sensing (Huete, 2016), and will be particularly noticeable in semiarid  
267 areas where the amount of precipitation will have a large impact on the local ecosystems.

268

269 Climate change and land disturbance initiate succession (e.g. primary succession and secondary  
270 succession), which is defined as the process the structure of a biological community changes over  
271 time (Huston and Smith, 1987). Primary succession is the process that plants and animals colonize a  
272 barren habitat for the first time, which could take hundreds of years. On the other hand, secondary  
273 succession begins after a major disturbance that transformed the original landscape, and if this land is  
274 undisturbed for some time, the evolving biological community will reach a stable ecological structure  
275 again. As remote sensing has a relatively short history, and the longest earth observation satellite,  
276 such as Landsat, only has a half-century record, it is not ideal to quantify primary succession, and  
277 there are only limited studies on this topic (e.g., Knoflach et al., 2021 and Lawrence, 2005).

278 However, remote sensing data have been frequently used for quantifying secondary succession after  
279 disturbance, which is usually called post-disturbance recovery or vegetation regrowth (Bartels et al.,  
280 2016; Zhao et al., 2016). Basically, we can quantify the rate of recovery using the slope of the  
281 vegetation index calculated based on remotely sensed time-series observations, and the larger the  
282 positive slope in a vegetation index the quicker the recovery.

283

284 Observing and monitoring places where disturbance, climate, and succession occurred is important,  
285 but what is more critical is to identify the specific change agent, and this effort is sometimes called  
286 change agent characterization (or attribution) in remote sensing. Among the variety of possible land  
287 change agents, we can divide them into direct or proximate causes (e.g., agriculture practice, urban  
288 development, fire, harvest, etc.) and distal or underlying driving forces (e.g., human population  
289 dynamics, human attitudes and behavior, economic transformation, climate change, etc.) (Geist and

290 Lambin, 2002; Lambin et al., 2001). Majority of the remote sensing studies are only focusing on  
291 creating change agents maps of the proximate causes, in which some of them are more focused on  
292 anthropogenic agents (Kennedy et al., 2015; Shimizu et al., 2019) and others are more of a natural  
293 agent focus (Oeser et al., 2017; Schroeder et al., 2017). Most of the remotely sensed change agent  
294 types are quite broad, and some of the typical categories include *agriculture practice, forest harvest,*  
295 *urban development, insect, wind, fire, hydrology, and vegetation stress.* Satellite time series  
296 observation collected before, during, and/or after the disturbance events and supervised machine  
297 learning classifiers are usually used together for change agent classification (Shimizu et al., 2019),  
298 and the inclusion of spatial domain of remote sensing data are frequently found helpful in improving  
299 separation of different change agents (Kennedy et al., 2015; Sebald et al., 2021; Shimizu et al.,  
300 2019). It should be noted that remote sensing of change agent is never an easy task. Changes of  
301 different agents can happen simultaneously or in close proximity to each other, which makes  
302 untangling these agents extremely hard sometimes (e.g., understory fire following by a pest  
303 infestation in forests). Moreover, different disturbance agents may result in the same or similar  
304 mechanism (for example, windstorms, wildfire, insect infestation, and drought will all lead to  
305 defoliation), which makes the spectral change signature very similar among the different agents.  
306 Additionally, high-quality change agent training data is extremely hard to collect consistently at  
307 large-scales. Unlike land cover training data that can be interpreted from any high-resolution remote  
308 sensing image, it is much hard to find training data of land change, and it is even more difficult to  
309 interpret the causality of the change based on the remotely sensed data alone (Pengra et al., 2020).  
310 Synthesizing all the land change agent related open data, such as the Land Change Monitoring,  
311 Assessment, and Projection (LCMAP) reference sample (Pengra et al., 2020), LANDFIRE reference  
312 data (Rollins, 2009), USGS Land Cover Trends data (Loveland et al., 2002), USFA National Insect  
313 and Disease Survey database (Johnson and Wittwer, 2008), NASA Cooperative Open Online  
314 Landslide Repository (COOLR) Landslide data (Kirschbaum et al., 2010), NOAA Severe Weather

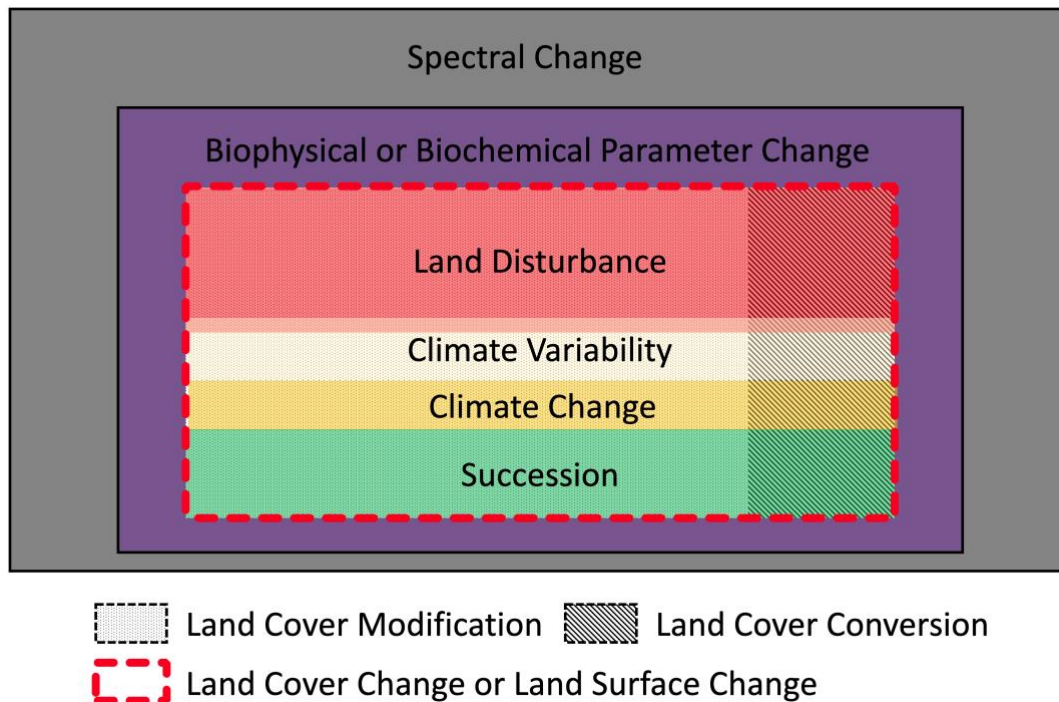
315 Data Inventory (SWDI) (NOAA, 2022), and Monitoring Trends in Burn Severity (MTBS) data  
316 (Eidenshink et al., 2007), and refining training data based on prior knowledge of change agent  
317 characteristics could be a potential solution. Remote sensing can also help better understanding the  
318 underlying driving forces behind global land change based on qualifying and quantifying human-  
319 environment interaction at multitude of spatial and temporal scales (Pricope et al., 2019). By  
320 integrating socioeconomic data with remotely sensed data and incorporating models (e.g., fixed-  
321 effects statistical) that are widely used by social scientists, it is possible to provide deeper  
322 understanding of the complex land change transitions and teleconnection/telecoupling (Friis et al.,  
323 2016; Lambin et al., 2001; NRC, 1999, 1998; Pricope et al., 2019; Seto et al., 2012)

324

### 325 **3 Relationship of various kinds of change terminologies**

326 A variety of change terminologies have been introduced for remote sensing of land change. Though  
327 they are all related to land change, their relationship is rather complicated and confusing. Fig. 4  
328 illustrates the relationship of some widely used land change terminologies, including spectral change,  
329 land surface change, land cover change, land cover modification, land cover conversion, land  
330 disturbance, climate variability, climate change, and succession, and biophysical/biochemical  
331 parameter change. Spectral change (the grey rectangle in Fig. 4), defined as the temporal changes in  
332 remote sensing spectral value, has been widely used in many remote sensing change detection studies  
333 (Cohen and Goward, 2004; Coppin and Bauer, 1996; Verstraete and Pinty, 1996). Spectral change is  
334 the broadest of all land change terminologies that could include all kinds of land changes (e.g.,  
335 changes caused by vegetation phenology and abrupt/gradual land surface changes), as well as  
336 spectral changes that have nothing to do with land change on the ground, such as atmospheric  
337 influences and data noises. On the other hand, land surface change (the region within red dashed line  
338 rectangle in Fig 4 that is also shared with land cover change) has also gained a lot of visibility in

339 remote sensing studies of land change (Brown et al., 2020; de Beurs et al., 2015; Sohl et al., 2004;  
340 Woodcock et al., 2020; Zhu and Woodcock, 2014), which usually includes all land change (e.g., all  
341 kinds of land cover conversions and modifications) that occurs on the Earth's surface, except for  
342 cyclic changes that are caused by vegetation phenology. As cyclic changes from vegetation  
343 phenology can also lead to biophysical/biochemical parameter changes, biophysical/biochemical  
344 parameter change (the purple rectangle in Fig. 4) includes land surface change (or land cover  
345 change), that will inevitably lead to changes in certain biophysical/biochemical parameters), as well  
346 as cyclic seasonal changes that cause changes in LAI and leaf chlorophyll contents. Land disturbance  
347 (the light red rectangle in Fig. 4), defined as any discrete event that occurs outside the range of  
348 natural variability of the land surface, if severe enough, can lead to land cover conversion, and is  
349 sometimes overlapped with climate variability (e.g., drought). Climate variability (the light yellow  
350 rectangle in Fig. 4) and climate change (the dark yellow rectangle in Fig. 4) are driven by the mean  
351 and variability of temperature, precipitation, or wind, and climate variability refers to the short-term  
352 variations in climate patterns (e.g., months, seasons, or years) and climate change refers to the long-  
353 term changes (e.g., decades or centuries). Both can lead to land cover conversion when it is persistent  
354 or have a significant impact on the land surface. Succession (the green rectangle in Fig. 4), defined as  
355 the process of the structure of a biological community changing over time can also change the land  
356 cover categories (e.g., transitioned from grass to shrub, and all the way to forest) with enough time  
357 and adequate recovery speed (Brown et al., 2020). Note that land disturbance, climate variability,  
358 climate change, and succession may all lead to categorical land cover change -- land cover  
359 conversion (the rectangles filled with stripes in Fig. 4), but most of the time they will only lead to  
360 within-state modifications or condition change -- land cover modifications (the rectangles filled with  
361 dots in Fig. 4), such as changes in the value of a certain biophysical/biochemical parameter.



362

363 **Fig. 4.** Relationship of some widely used land change terminologies, including spectral change, land  
 364 land surface change, land cover change, land cover conversion, land cover modification, land disturbance,  
 365 climate variability, climate change, succession, and biophysical/biochemical parameter change.  
 366

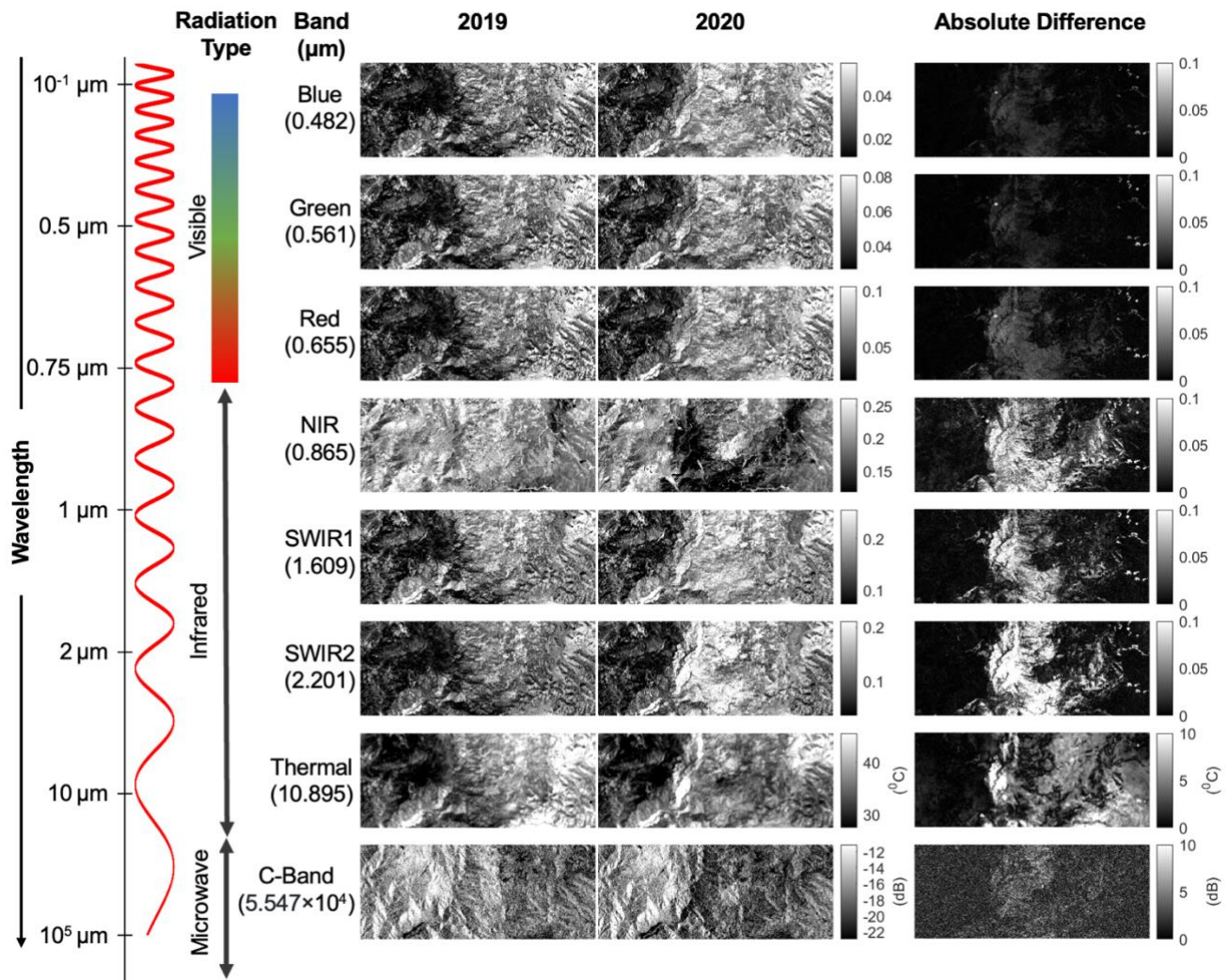
367 **4 The spectral, spatial, temporal, and angular issues in detecting land change**

368 If the remote sensor is designed perfectly at the right spectral, spatial, temporal resolutions and  
 369 viewing angles, all land changes should show up with large magnitudes of spectral change. However,  
 370 this is never the case in reality, and issues from spectral, spatial, temporal, and angular domains will  
 371 all greatly impact the remote sensing platform's capability of detecting land change.

372 **4.1 The spectral issues**

373 The spectral values record the amount of electromagnetic energy in specific wavelengths, such as  
 374 visible, Near Infrared (NIR), Short-Wave Infrared (SWIR), thermal, and microwave bands. Remote  
 375 sensing of land change assumes that different land surfaces will have different spectral values, and if  
 376 we difference the spectral values collected at different time points, we can identify the change. In  
 377 practice, the different land surfaces may share the same or similar spectral values for certain spectral

378 bands, and if the spectral bands that can separate the two different kinds of land surface do not exist  
379 in the remote sensing bands, there will be no way to detect changes occurred between the two land  
380 surface types. For example, when forests are burned, the changes in visible bands, such as Blue,  
381 Green, and Red, and certain microwave bands (e.g., C-Band) are usually very subtle (Fig. 5) and if  
382 those bands are used for detecting burned areas, it would be extremely hard for any kind of change  
383 detection algorithms. However, large differences will usually show in NIR, SWIR1, SWIR2 bands  
384 (reduced vegetation and water content), and thermal band (higher temperature) after forest fire (Fig.  
385 5), and the burned areas can be easily detected if spectral bands within these four spectral ranges  
386 exist. Note that there are remote sensors that can provide many narrow spectral bands, and some of  
387 the bands, such as red edge bands (in the NIR band range), can provide new change information (e.g.,  
388 forest structure and health change) that the broadband cannot provide (Cho et al., 2012; Eitel et al.,  
389 2011).



390

391 **Fig. 5.** Spectral change before and after the land change caused by fire. The changes in visible bands  
 392 and microwave band are very subtle, but substantial in NIR, SWIR, and thermal bands. Blue, Green,  
 393 Red, NIR, SWIR1, SWIR2, and thermal bands are derived from Landsat 8 surface reflectance and  
 394 brightness temperature data, and microwave C-Band is from Sentinel-1 C-Band Synthetic Aperture  
 395 Radar data with dual-band cross-polarization (Vertical transmit/Horizontal receive) at descending  
 396 orbit. All the remotely sensed images were acquired at central latitude/longitude (40.100 /-120.607)  
 397 in June 2019 and 2020 and clipped to same extent of 1001 pixels by 401 pixels at 30 m spatial  
 398 resolution.

399

400 Additionally, the selection of the right spectral bands is particularly critical to identify the change  
 401 agent, change target, as well as to determine the specific change process. The spectral change values in  
 402 different bands, sometimes called spectral change vector, are the key variables for separate different  
 403 change agents, as both the change vector angle and change vector magnitude contain rich information  
 404 on the kind of change that is occurring (Lambin and Strahlers, 1994). On the other hand, the spectral

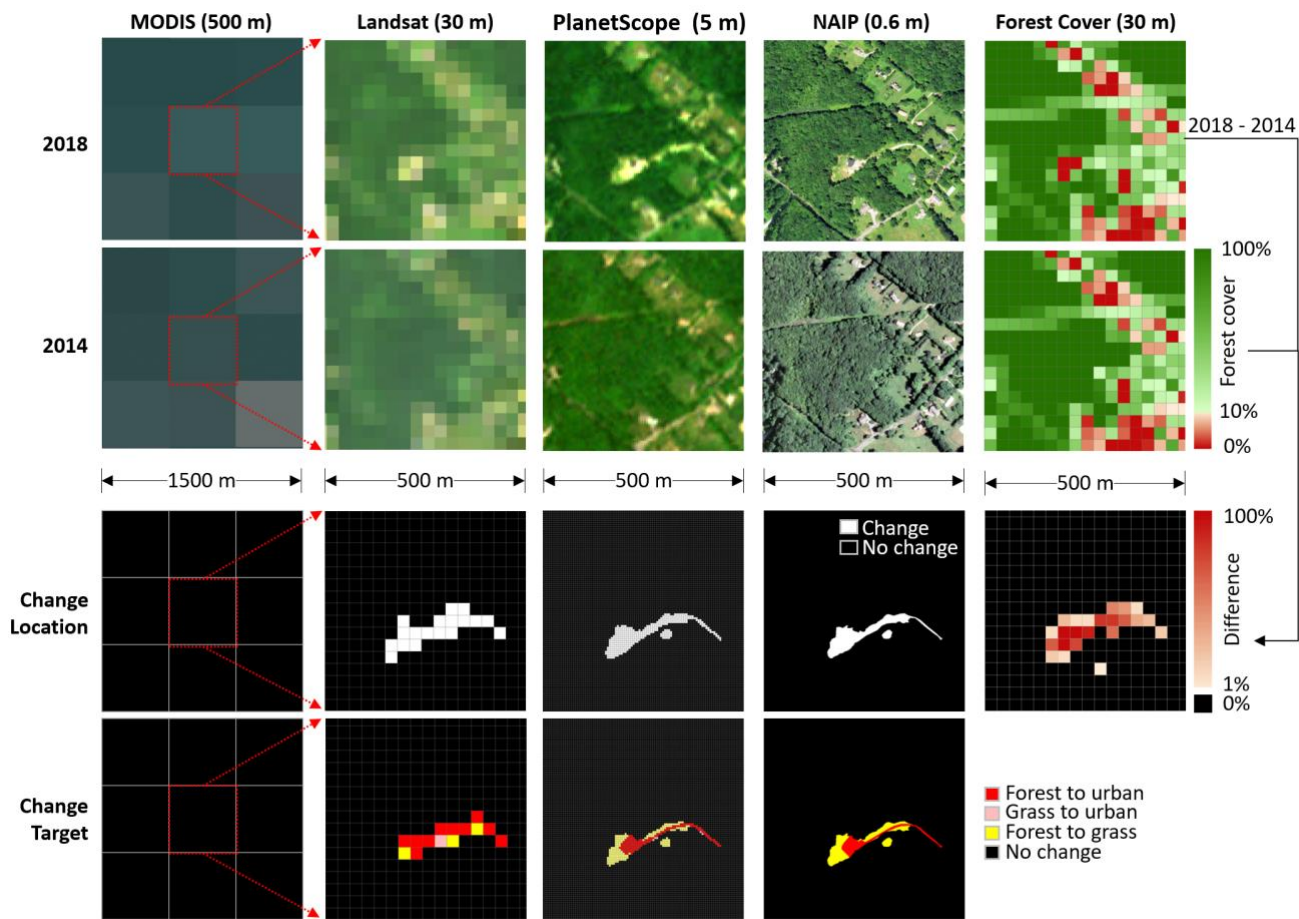
405 values before and after the change are the most important input variables for characterizing the  
406 change target. While given cover types may have similar and indistinguishable spectral responses at  
407 specific points in time, in most cases, the spectral behavior of different cover types varies over time,  
408 and the combined ability to look both multi-spectrally and multi-temporally should introduce  
409 evidence that can be used to discriminate different cover types. For land change process  
410 characterization, as the change vector magnitude is used directly to separate dramatic and subtle  
411 changes, the selection of the right spectral bands with the best capability to quantify the severity of  
412 change is extremely important.

413

## 414 **4.2 The spatial issues**

415 The spatial resolution, defined as the dimension in meters of the ground-projected Instantaneous-  
416 Field-of-View (IFOV), determines the minimum mapping unit on the ground (e.g., a Landsat 8 pixel  
417 covers 30x30 m<sup>2</sup> land area). Remotely sensed images from various kinds of platforms can provide a  
418 wide range of spatial resolutions from sub-meters to tens of kilometers (Belward and Skøien, 2015).  
419 Remote sensing data with the higher spatial resolution are generally preferred as the input for change  
420 detection, as the higher the spatial resolution, the better the capability in detecting small-scale land  
421 changes (Coppin et al., 2004). However, when the spatial resolution is too high (e.g., < 1 meter), the  
422 shadow from the land surface objects will start to show up (Bruzzone and Vovolo, 2012), and the  
423 trade-off between spatial and temporal resolutions will make it extremely hard to find another revisit  
424 image unless it is pointed to the same location after changing its view angle, which will cause artifact  
425 again due to the large view angle difference in the image. On the other hand, if the spatial resolution  
426 is too coarse, not only small-scale changes will not be able to show up in satellite signals (see the  
427 MODIS images in Fig. 6), but also the large difference in point-spread-function and BRDF impact  
428 will make change signals easily buried in the data noise (Xin et al., 2013). Therefore, most of the

429 remotely sensed data used for land change studies are based on medium resolution satellites with  
 430 resolution between 10–100 meters, such as SPOT, Sentinel-2, and Landsat (Martin and Howarth,  
 431 1989; Szostak et al., 2018; Zhu, 2017), and the coarse resolution data, such as MODIS and AVHRR  
 432 are mostly used to extract gradual change based on long time series data (Myneni et al., 1997; Zhu et  
 433 al., 2016).



434

435 **Fig. 6.** The impact of spatial resolution on maps of change location and change target between 2014  
 436 and 2018. All the remotely sensed images were acquired at central latitude/longitude (41.781/-  
 437 72.234) in summer 2014 and 2018 and reprojected into the WGS84 UTM Zone 19N. The MODIS,  
 438 Landsat, and PlanetScope satellites provide remote sensing images at coarse resolution (500 m),  
 439 medium resolution (30 m), and high resolution (5 m), respectively. The National Agriculture Imagery  
 440 Program (NAIP) data are aerial photos, that can be considered as a reference of the land changes at  
 441 0.6 m resolution. The change location and change target maps are derived from MODIS, Landsat,  
 442 PlanetScope, and NAIP images, respectively. Changes are detectable when >10% of the pixel  
 443 changed. Forest is defined as pixels with >10% coverage of trees, and urban is defined as pixels  
 444 with >10% coverage of built areas. None of the changes are detectable from MODIS images (500 m),  
 445 but detectable at the other remote sensing images at 0.6-30 m spatial resolutions. Note that due to the

446 difference in spatial resolution, the change location and change target maps are all different,  
447 particularly when the pixel size is larger than 30 m.  
448

449 Land changes are usually occurring at small scales. When the pixel size is relatively large, pixels  
450 mixed with multiple land cover types happen frequently, and changed areas smaller than the pixel  
451 size are also seen very often. Therefore, a lot of time, land change may only occur on a small fraction  
452 of a pixel (the fraction is a continuous variable), which may not match well with categorical change  
453 maps, such as change/stable (change location) and land cover change (change target) maps (Fig. 6).  
454 Usually, a threshold is introduced to determine whether a pixel has changed or not. For example, in  
455 Hansen et al. (2013), forest change is defined as a pixel with more than 50% change in forest cover  
456 within a pixel. On the other hand, the definition of land cover also plays a major role in determining  
457 whether there is a land cover conversion or not after the change event. For example, if a forest pixel  
458 is defined as a pixel with more than 10% of tree cover, and grass land is defined as a pixel with more  
459 than 10% of grass cover, land cover conversion from forest to grass will happen only if more than  
460 90% of the trees are removed for a fully forested pixel (Fig. 6). The situation could be different if  
461 some proportion of forest is converted to built-up lands. This is because land cover definition is  
462 usually resources driven, and certain classes will have a higher priority than the other classes in the  
463 classification system (e.g., urban > forest > grass), and when there are multiple cover types present in  
464 the same pixel, it will be labeled as urban or developed even if it covers a small proportion of the  
465 pixel (e.g., > 10%) (Pengra et al., 2020). In this case, if within a fully forested pixel, more than 10%  
466 of trees have been removed, and a new house is established to cover that area, even with the  
467 remaining forest cover slightly less than 90%, this pixel is still considered to have gone land cover  
468 conversion (from forest to urban) (Fig. 6).

469

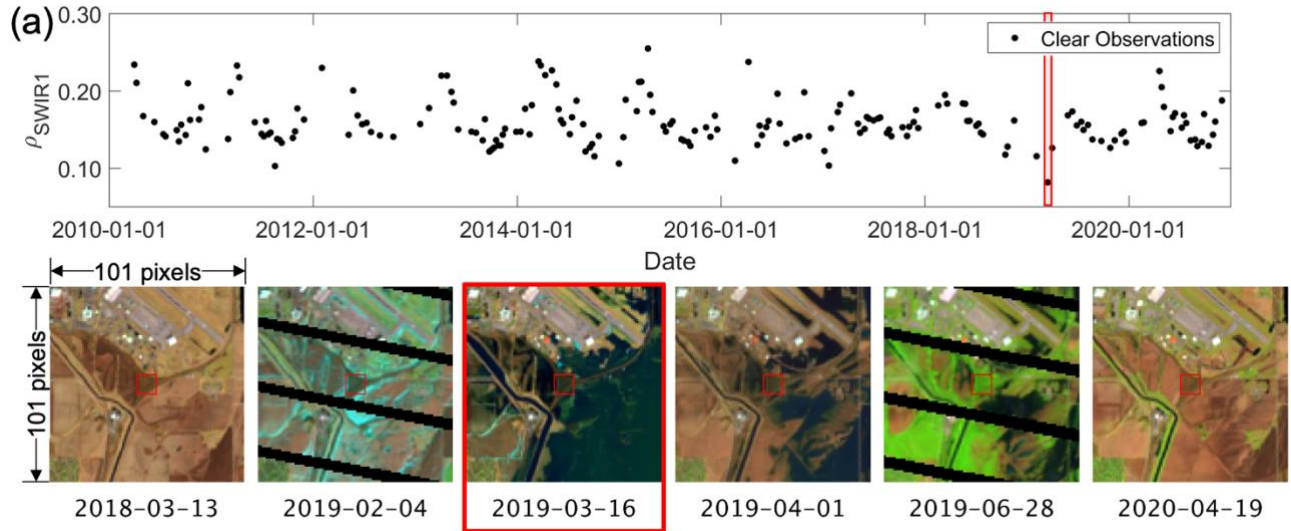
### 470 **4.3 The temporal issues**

471 The temporal resolution of a remote sensing system refers to how often the remote sensor records  
472 imagery of a particular area (e.g., Landsat 8 visits the same location every 16 days), and there are  
473 remote sensing systems that can collect observations every minute, hours, daily, weekly, monthly,  
474 and a few years (Jensen, 2009). The temporal resolution of the remote sensing data plays a major role  
475 in determining the change time, improving detection of change location, and at the same time  
476 providing rich information in detection of change process, agent, and target.

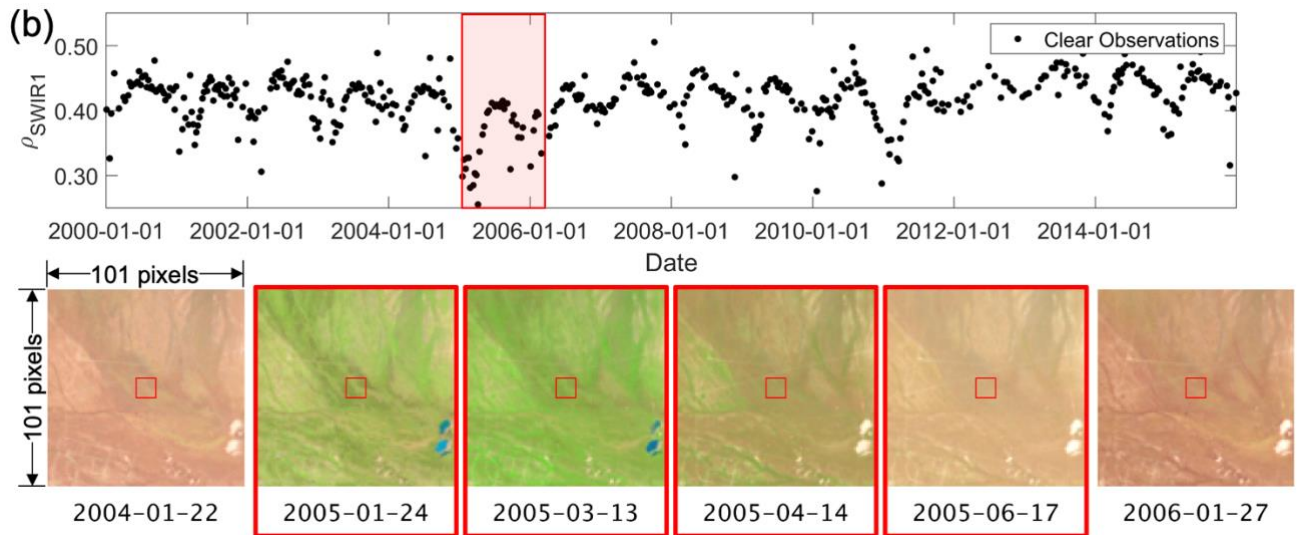
477  
478 Essentially, more accurate detection of change time could be achieved based on observations of  
479 higher temporal resolutions, as change time can be contained within a narrower time interval, and this  
480 has been echoed by the fact that remote sensing change detection algorithms are using denser time  
481 series (Zhu, 2017). The revisit time of remote sensing data should be shorter than the lasting time of  
482 the change event to be able to detect the change we are interested in, otherwise, these change events  
483 may already be fully recovered before the next visit of remote sensors. For example, with two sensors  
484 working simultaneously, Landsat time series can provide 8 days revisit observations for the same  
485 location if we do not consider observations blocked by cloud, cloud shadow, and snow/ice. For  
486 ephemeral change such as floods that only last a few days, it is less likely to be observed based on  
487 Landsat time series alone (Fig. 7a). In Fig. 7a, we are lucky enough to have one clear Landsat image  
488 located during the flooding, but if it is blocked by clouds, there is no way to detect this kind of  
489 ephemeral changes, even if we used all available Landsat time series. For grassland change (i.e.,  
490 abrupt greenness change) caused by climatic variability and forest change caused by beetle  
491 infestation, they can last for a year or multiple years, respectively, and are usually detectable if  
492 annual Landsat observations are used (Fig. 7b-c). Another extreme is that for urban development  
493 related changes (Fig. 7d), they are usually more permanent, and Landsat data that are 5 or 10 years  
494 apart are still able to capture them. Therefore, the minimum temporal resolution required for different

495 land change applications is usually quite different, and the denser the time series observations used,  
496 the more accurate in detection of the time and location of change.

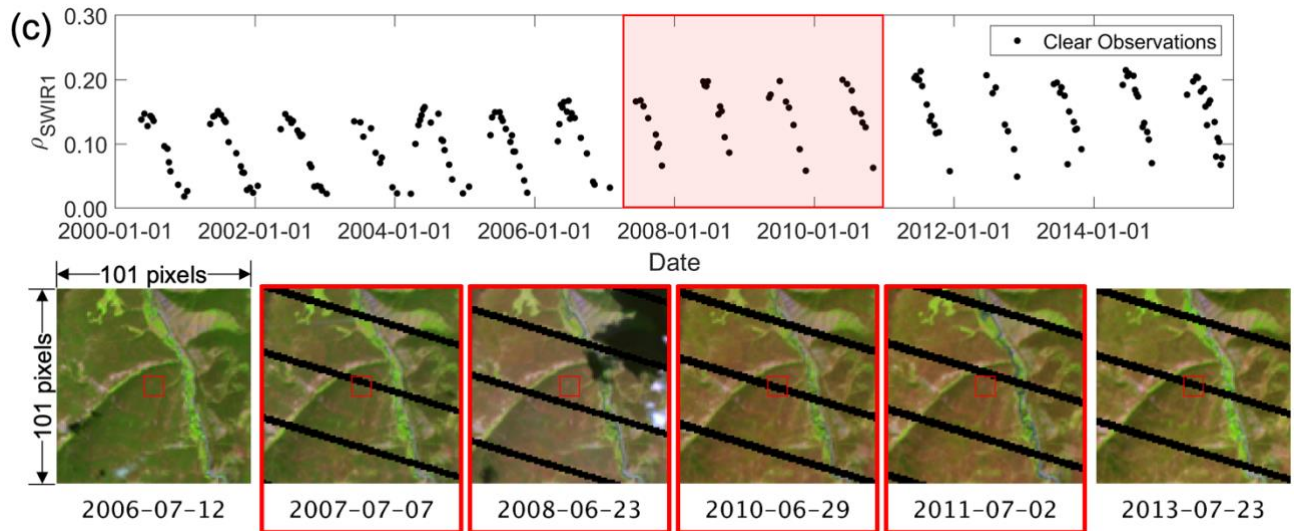
497



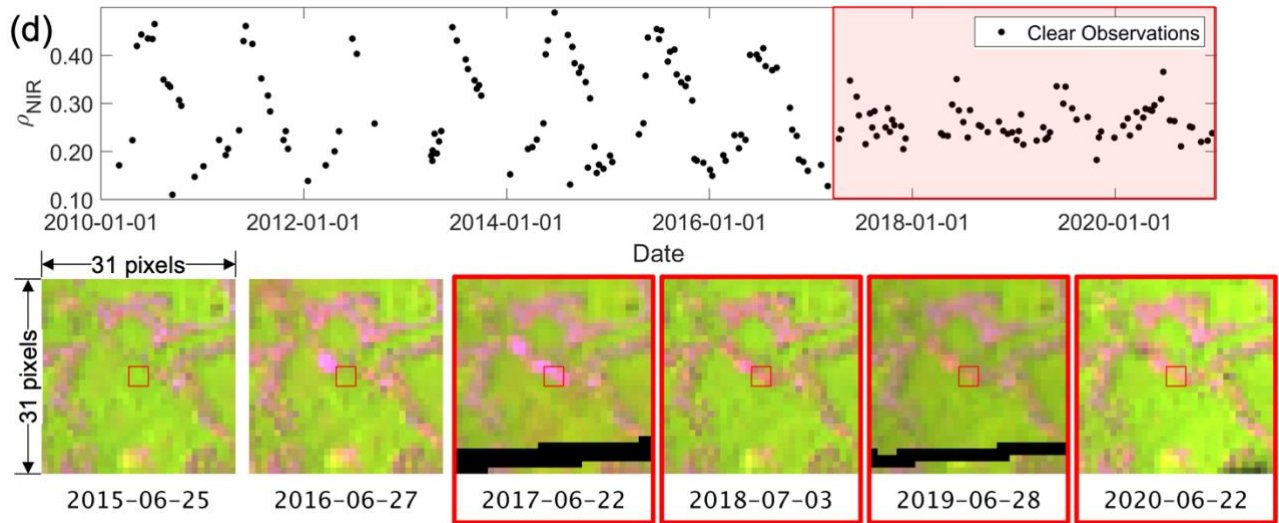
498



499



500



501

502 **Fig. 7.** The impact of temporal resolution on land change detection. (a) A flood event that lasted for a  
 503 few days at central latitude/longitude (41.103/-95.906). Of all the available Landsat observations,  
 504 only a single observation can observe this ephemeral event. (b) Climatic variability over grassland  
 505 that lasted almost a year at central latitude/longitude (34.838/-117.460). (c) Beetle infestation related  
 506 land change that lasted for several years at central latitude/longitude (40.226/-106.064). (d)  
 507 Urbanization over forested areas located at latitude/longitude (41.70/-71.57). In each figure, the time  
 508 series plot in the upper panel is derived from all available Landsat observations at the center of the  
 509 smaller red square of the false color composited images at the lower panel. The change period is  
 510 highlighted by the red rectangles in the upper panel and the larger red rectangle surrounding the false  
 511 color composited images in the lower panel. The false color composited images are shown in Landsat  
 512 SWIR1, NIR, and Red bands, and they are directly comparable because of the same stretch display.  
 513 Some of the images have black stripes which are due to the Landsat 7 Scan Line Corrector-off issue.

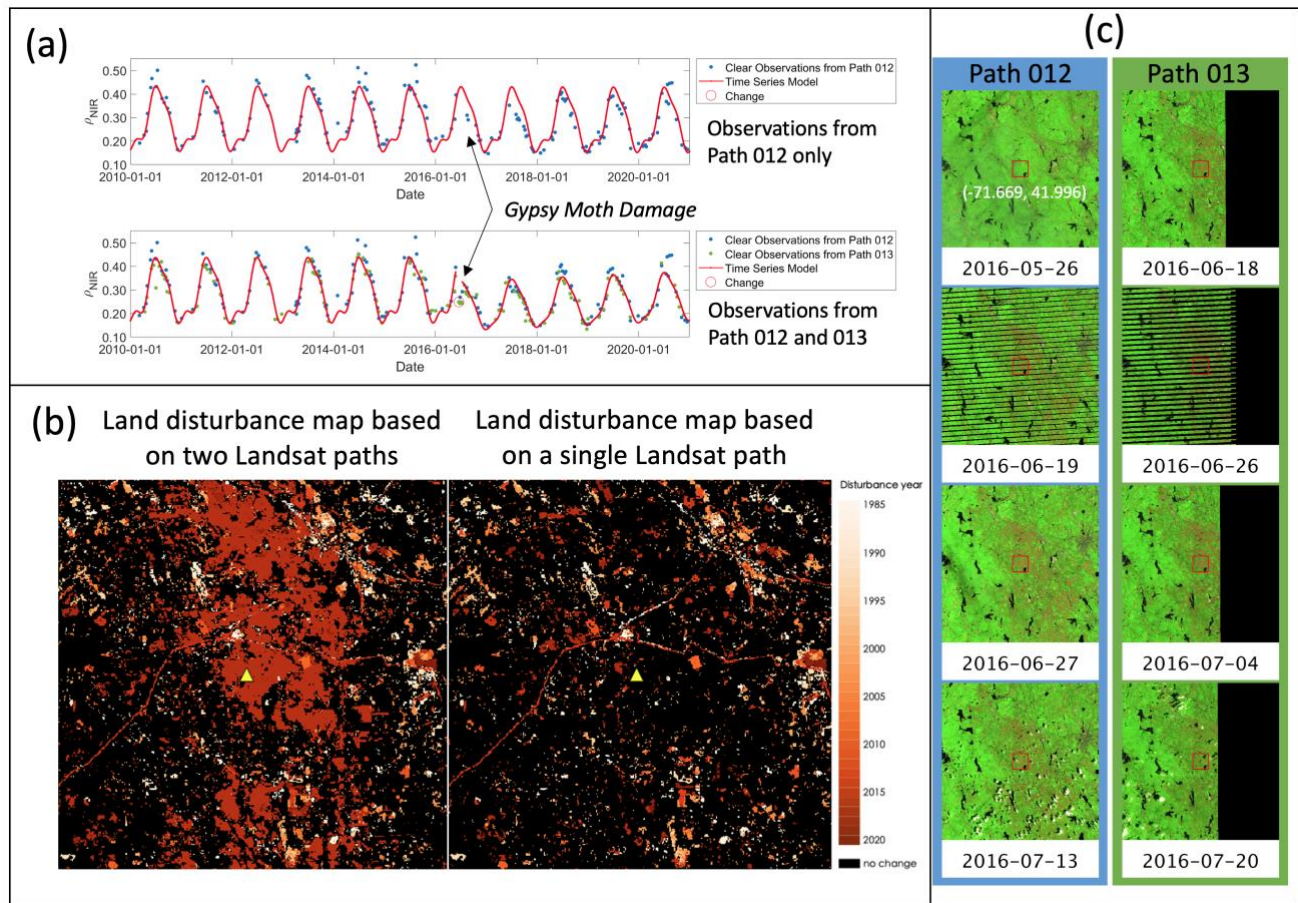
514

515

516 The use of dense time-series observations could also introduce issues in change detection, as for  
517 ephemeral changes that last for a short time, only observations with temporal resolutions higher than  
518 the time interval of ephemeral changes can capture this kind of land change. Therefore, changes  
519 detected based on the dense time series will be different when remote sensing data of different  
520 temporal resolutions are used, and usually, the denser the time series, the more changes will be  
521 detected. Even if a single remote sensing system is used (e.g., Landsat), the time series may have  
522 different temporal resolutions at different places and at different times due to the overlap of adjacent  
523 swaths, the presence of cloud or snow/ice, and the data acquisition strategies (Brown et al., 2020;  
524 Zhu et al., 2018). For example, Gypsy Moth infestation usually only lasts for one or two months, and  
525 if all available Landsat data is used, we can have around four clear observations (without using  
526 observations from the neighboring path) in two months for most places (assume cloud cover is 50%).  
527 In certain places where two Landsat paths overlap with each other (the overlap areas), we could have  
528 around eight clear observations, and if we use more than four consecutive observations to confirm a  
529 change, this land change can only be detected in the overlap areas (Fig. 8a). The use of overlap path  
530 observations brings new science capability for Landsat data, but also brings inconsistency to the final  
531 land change maps (between the overlap and non-overlap areas). This is particularly problematic for  
532 large-scale remote sensing change products, as large differences in land change patterns will show up  
533 both spatially and temporally. Methods that select data from the same path or adjust the number of  
534 observations to confirm change based on data density could be possible solutions to alleviate this  
535 issue, but it is at the sacrifice of losing the temporal density for certain places, which may lead to  
536 omission errors (Fig. 8b). Moreover, the time-series observations collected at different temporal  
537 density and irregularity can also impact the accuracies of change detection algorithms that rely on  
538 dense time-series observations, making detection accuracy differ for different locations and dates  
539 (Zhang et al., 2021).

540

541 Additionally, the use of dense time series can create new information or more accurate change  
542 information that the traditional two-date image difference method cannot provide. For example, we  
543 can get to know how this change is occurring or the change process based on the trend of the time  
544 series, the change magnitude, and the duration of the change. The information embedded in the time  
545 series data provides important spectral-temporal information of the pixel and we can extract this  
546 information based on estimated time series model coefficients and statistical metrics to provide a  
547 more accurate classification of change target (Zhu, 2017). These derived spectral-temporal metrics  
548 could even revolutionize the current land cover classification system and bring in new land cover  
549 categories that are continuous in time and embedded with changing conditions, such as *greening*  
550 *urban, young forest, mature forest, declining forest* (Zhu and Woodcock, 2014). Finally, the time  
551 series before, during, and after land change all contain rich spectral-temporal information on the  
552 change agent and could be used as major input for change agent classification.



554

555 **Fig. 8.** A comparison of change detection results caused by Gypsy Moth damage using two Landsat  
 556 paths (or swaths) data and a single path data. (a) Landsat NIR surface reflectance observations at the  
 557 center of the red square of the false color composited images on the right (c) at central  
 558 latitude/longitude (41.996/-71.669). The blue dots are from the Landsat path #12 and green dots are  
 559 from the path #13. The red line is the estimated time series model, and the red circle is the land  
 560 surface change captured by the COLD algorithm with six consecutive observations to confirm a  
 561 change (Zhu et al., 2020). (b) Land disturbance map created based on the COLD algorithm using  
 562 Landsat observations from two paths and a single path (#12). The darker the color, the more recent  
 563 the land disturbance detection. (c) The false color composited Landsat images from the path #12 (in  
 564 blue outlines) and the path #13 (in green outlines) were shown in SWIR1, NIR, and Red bands, and  
 565 they are directly comparable because of the same stretch display. This figure demonstrated that for  
 566 places with two Landsat paths coverage, Gypsy Moth damage is possible with the COLD algorithm,  
 567 but not possible for places with only a single Landsat path coverage. COLD: Continuous monitoring  
 568 of Land Disturbance.  
 569

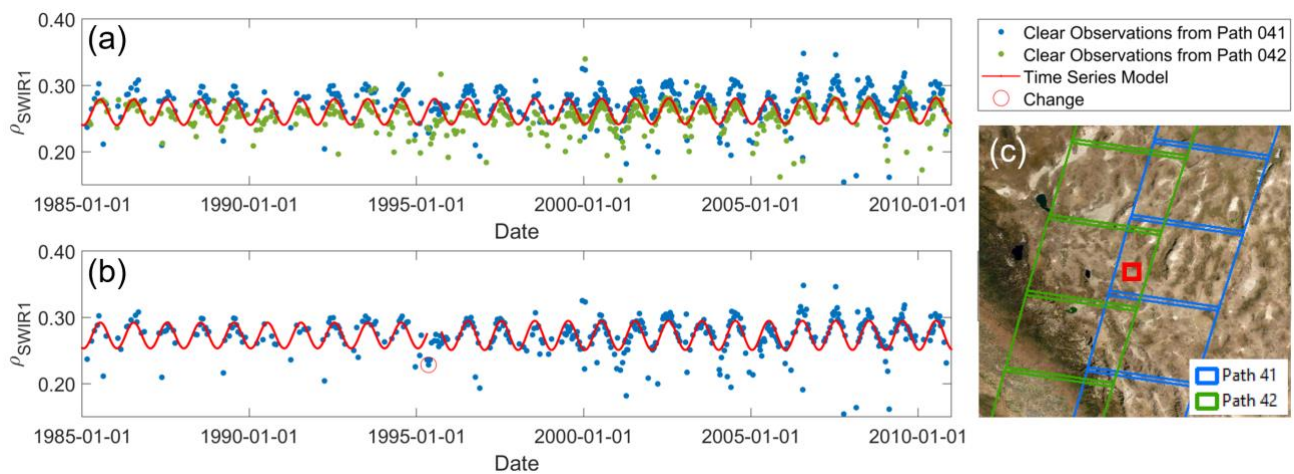
570 In addition to the repeating frequency, the time of day the remote sensing observations are collected  
 571 is also helpful for better understanding different facets of land change. For example, most of the time  
 572 series we discussed are remotely sensed data collected during the daytime (e.g., around 10 am),

573 which relies on the reflected electromagnetic radiation from the sun. There is also satellite data with a  
574 high signal-to-noise ratio that can take images at nighttime, which can provide unique information on  
575 human activities, as most of the nighttime lights are from artificial lights. Time-series nighttime light  
576 data have been widely used to monitor anthropogenic-related land change and usually at a large  
577 scale. However, as there are also other sources of light at night, such as moonlight, aurora, lighting,  
578 the use of dense time series of nighttime light data are still very rare (Wang et al., 2021), and the  
579 densest time series data ever used is still the average monthly or yearly nighttime light observations  
580 (Elvidge et al., 2021; Levin and Noam, 2017). Recently, NASA has created a Black Marble product  
581 that has corrected most of these nonhuman-activity-related light sources and has provided the  
582 potential of using daily nighttime light observations for land change studies (Román et al., 2018).

#### 583 **4.4 The angular issues**

584 The energy recorded by the remote sensing systems contains very specific angular characteristics,  
585 which is a function of illumination source (e.g., Sun for a passive system or the sensor itself for  
586 active systems) angles and the sensor viewing angles, known as the Bidirectional Reflectance  
587 Distribution Function (BRDF) (Schaaf et al., 2002). This bi-directional nature of remote sensing  
588 systems will cause differences in the sensor collected radiance, as well as influence the calculation of  
589 surface reflectance, which are some of the major “noise” sources in detecting change locations (Xin  
590 et al., 2013). Even for some of the sensors that only collect near nadir observations, such as Landsat,  
591 the changes in the solar angles and view zenith angles (mostly for observations collected in overlap  
592 swaths) will still cause large reflectance differences (Qiu et al., 2019a; Zhang et al., 2018), and  
593 potentially lead to omission or commission errors in change detection (Fig. 9a). Fortunately, with  
594 enough remote sensing observations collected at the different view and solar angles within a short  
595 time, this BRDF function can be modeled, and local-noon nadir observation can be estimated for  
596 some coarse resolution satellites, such as MODIS and VIIRS (Liu et al., 2017; Schaaf et al., 2002),

597 and these BRDF parameters can help reduce BRDF effect in medium resolution satellites, such as  
 598 Landsat and Sentinel-2 (Claverie et al., 2018; Roy et al., 2016). Other solutions such as selecting  
 599 observations within the same swath and creating time series models that estimate the solar angle  
 600 difference along with vegetation phenology changes can also remove or reduce the BRDF differences  
 601 embedded in the satellite data, and in this way, the change pixel can be correctly identified (Fig. 9b)  
 602 using a time-series based change detection algorithm (Zhu et al., 2020). It is worth noting that the  
 603 angular information can be useful for identifying the target and location of land change, such as  
 604 improving land cover classification (Jiao et al., 2011), detecting moving objects such as cloud (Frantz  
 605 et al., 2018), aircraft (Liu et al., 2020), and detection of newly built houses (Huang et al., 2020), due  
 606 to the inclusion of 3D information.



607

608 **Fig. 9.** The impact of BRDF on land change detection. (a) Change detection using all observations  
 609 collected in overlap paths. The BRDF effect, dominated by the different sensor view angles from two  
 610 adjacent paths, results in an omission error. (b) Change detection using all observations in a single  
 611 path with minimum view zenith angle. The change caused by climate variability can be successfully  
 612 detected when the BRDF effect is reduced in time series observations collected from a single swath.  
 613 (c) Landsat Path/Row tiles. The blue and green polygons indicate the Landsat path #41 and #42,  
 614 respectively. The center of the red square indicates the location of the time series plots (a) and (b)  
 615 at latitude/longitude (38.737/-117.880). This change detection example is generated from all available  
 616 Landsat time series and a time-series-based change detection method called COLD (Zhu et al., 2020).  
 617 COLD: Continuous monitoring of Land Disturbance.

618

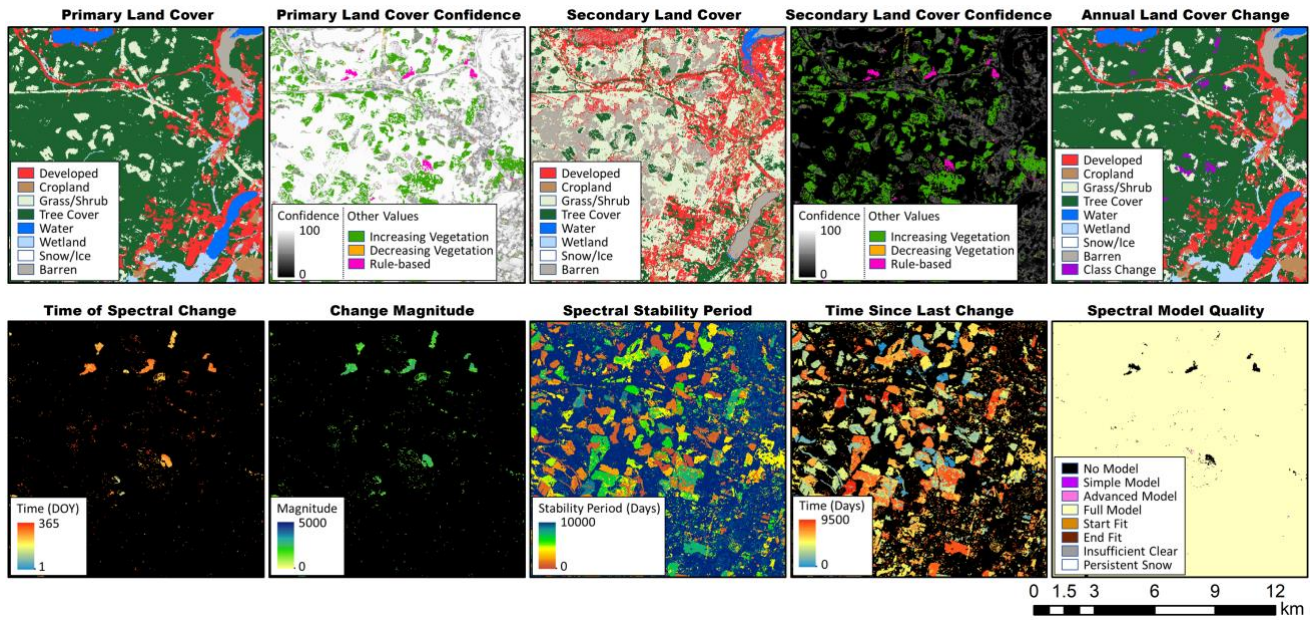
619 **5 Current land change products**

620 Lots of remote sensing-based land change products have been created, and some of them have been  
621 widely used for a variety of fields, such as environmental sustainability, land management,  
622 biodiversity conservation, and ecosystem health assessment. However, most of these land change  
623 products are only focusing on three facets of land change – the location, time, and target of change  
624 (mostly land cover), and very few products are trying to provide some of the other facets of land  
625 change, such as change agent or change process (Table 1). Most of these products are relying on  
626 medium resolution images (<30 m) and dense time-series observations (e.g., yearly, or monthly, or  
627 even weekly observations).

628  
629 Most of the current large-scale land change products are only focusing on a single change target, such  
630 as changes in *forest*, *urban*, or *water* (Table 1). For instance, Hansen et al. (2013) created the 2000-  
631 2012 global 30-m forest cover and forest cover change (i.e., forest loss and forest gain) products  
632 based on time series spectral metrics of Landsat data, and a supervised classification approach. The  
633 North American Forest Dynamics (NAFD) project implemented the Vegetation Change Tracker  
634 (VCT) algorithm (Huang et al., 2010) to produce annual forest disturbance maps for the  
635 conterminous United States (CONUS) from 1986 to 2010 based on annual Landsat time series data  
636 (Zhao et al., 2018). Liu et al. (2020) created 30-m Global Annual Urban Dynamics (GAUD) dataset  
637 for providing information on urban expansion and green recovery from 1985 to 2015 based on  
638 existing global urban extent maps and Landsat time series data. European Space Agency (ESA)  
639 produced the Global Human Settlement Layer (GHSL) for multiple years, which can provide new  
640 global spatial information, evidence-based analytics and knowledge describing the human presence  
641 such as built-up area and population distribution on the Earth (Pesaresi et al., 2016). The ESA Global  
642 Surface Water (GSW) dataset provides different facets of the spatial and temporal distribution of  
643 surface water over long time periods at a 30-meter resolution based on 30+year Landsat data, such as  
644 water occurrence for presenting overall water dynamics, water recurrence for describing how

645 frequently water returned from one year to another, and water seasonality for capturing the intra-  
646 annual dynamics of water surfaces (Pekel et al., 2016). This dataset also includes water occurrence  
647 change intensity maps between two epochs (1984 to 1999, and 2000 to 2020), which can provide  
648 information on where surface water occurrence increased, decreased, or remained the same. In  
649 addition, products of single change agent are available as well, particularly for fire. For example,  
650 Giglio et al. (2018) applied dynamic thresholds of a burn sensitive vegetation index composite data  
651 (derived from daily 500 m MODIS time series) to generate global burned area product, in which the  
652 date of burn area will be provided within each individual MODIS tile with 10 degrees by 10 degrees.  
653 Only a few products can provide information on land change on different kinds of land surfaces. The  
654 National Land Cover Database (NLCD) provides multi-temporal land cover and land cover change  
655 products for CONUS, Hawaii, Alaska and Puerto Rico between 2001 and 2019 for every 2-3 year  
656 interval, based on decadal Landsat data as well as other ancillary datasets (Jin et al., 2019). Using  
657 daily seamless data cubes generated from multi-source remote sensing data, Liu et al. (2021)  
658 generated 30 m resolution global land cover map data for 36 years by combining strategies of sample  
659 migration, machine learning, and spatio-temporal adjustment, which can be used to study global land  
660 change. Among all these products, the newly released Land Change Monitoring, Assessment, and  
661 Projection (LCMAP) product is one of the few land change products that not only can provide  
662 change location and time (e.g., Time of Spectral Change product), change target (e.g., Annual Land  
663 Cover Change product), but also has products on land change process information (e.g., Change  
664 Magnitude, Time Since Last Change, and Spectral Stability Period products), through a suite of ten  
665 LCMAP science products (Fig. 10) (Brown et al., 2020). The list of products also demonstrated the  
666 difficulty of providing information on change agent at large-scales.

667



668

669

670

671

**Fig 10.** LCMAP Ten Individual Products. This example is derived from LCMAP product version 1.2 in 2010 at Washington state, U.S. LCMAP: Land Change Monitoring, Assessment, and Projection.

672 Table 1. A list of current large-scale land change products. Only the most recent literatures are listed here.

Product Name	Coverage	Change Location	Change Time (Period)	Change Target	Change Process	Change Agent	Satellite Data	Citation
Hansen forest change map	Global	30-meter	Annual (2000- 2019)	Forest gain Forest loss	N/A	N/A	Landsat	(Hansen et al., 2013)
Global Surface Water	Global	30-meter	Intra-annual Annual (1984-2020)	Water seasonality Water transitions Annual water recurrence	Water occurrence change intensity	N/A	Landsat	(Pekel et al., 2016)
MODIS burned area	Global	500-meter	Day of Year (2000-Present)	Burned area	N/A	Fire	MODIS	(Giglio et al., 2018)
NAFD-NEX	CONUS	30-meter	Annual (1986-2010)	Forest disturbance	N/A	N/A	Landsat	(Zhao et al., 2018)
GHSL	Global	30-, 250-, and 1000-meter	Multiple years (1975, 1990, 2000, and 2014)	Built-up area	N/A	N/A	Landsat	(Pesaresi et al., 2016)
NLCD	United States	30-meter	2-3 years (2001-2019)	Land cover change Forest disturbance	N/A	N/A	Landsat	(Jin et al., 2019)
GAUD	Global	30-meter	Annual (1985-2015)	Urban expansion Green recovery	N/A	N/A	Landsat	(Liu et al., 2020)
LCMAP	CONUS	30-meter	Annual Day of Year (1985-2019)	Land cover change Land spectral change	Change magnitude Spectral stability period Time since last change	N/A	Landsat	(Brown et al., 2020)
iMap	Global	30-meter	Annual Seasonal (1985-2010)	Land cover change	N/A	N/A	Landsat, MODIS, and AVHRR	(Liu et al., 2021)

673 Notes: CONUS: COnterminous United States; NLCD: National Land Cover Database; LCMAP: Land Change Monitoring, Assessment, and Projection; GHSL: Global  
674 Human Settlement Layer; GAUD: Global Annual Urban Dynamics; NAFD-NEX: North American Forest Dynamics - NASA Earth Exchange.

## 675 **6 Conclusion and future recommendations**

676 Land change science has made big advancements with the development of remote sensing  
677 technology, and questions of where, when, what, why, and how this change takes place can be fully  
678 evaluated and mapped. We proposed a new concept of the multifaceted view of land change through  
679 the lens of remote sensing and recommended five facets including change location, time, target,  
680 process, and agent. We also discussed the relationship of various kinds of land change terminologies  
681 including spectral change, land surface change, biophysical/biochemical parameter change, land  
682 disturbance, climate change, climate variability, succession, land cover change, land cover  
683 conversion, and land cover modifications, in which large differences were identified among these  
684 terminologies. The impact of spatial, spectral, temporal, and angular domains of the remotely sensed  
685 data on observation, monitoring, and characterization of land change was also evaluated. We  
686 emphasized the importance of selecting the “right” spectral bands and spatial resolution of remote  
687 sensing data for the specific land change problem. We discussed the benefits and challenges when  
688 dense time-series and multi-angle satellite observations are used for observing and characterizing  
689 land change. We also reviewed some of the current land change products, and observed the lack of  
690 products that provide multiple or full land change facets, particularly for the facets of land change  
691 agent and process.

692

693 Therefore, we have a few future recommendations on remote sensing of land change as follows.  
694 First, it is important to recognize the multifaceted nature of land change, and when remote sensing  
695 data are used to study land change, specifying which land change facet is being studied, is usually the  
696 first step. Second, remote sensing-derived land change products reported with all five facets are  
697 highly recommended, as land change can only be fully understood if they are viewed from all  
698 different angles. Third, we think a major shift on the focus from land target change to land process

699 and agent change detection are expected in future remote sensing studies, as these two facets are far  
700 less studied in remote sensing community, and why and how global land is changing are some of the  
701 most difficult and important science questions. Fourth, land change science has transitioned into  
702 more complex systems such as land system science (Turner et al., 2021), which requires deeper and  
703 more comprehensive land change information. For example, most of the current remote sensing  
704 change agent products are not detailed enough for social sciences to answer the question of “why”,  
705 and the combined use of socioeconomic data and more integrated social-environment theory could  
706 provide new and deeper insights (Tellman et al., 2020). Finally, we need to recognize that every  
707 remote sensing system has limitations and weaknesses in land change studies, and a thorough  
708 evaluation of all spectral, spatial, temporal, and angular issues is highly recommended.

709

## 710 **Acknowledgment**

711 This research was supported by the USGS-NASA Landsat Science Team Program for Toward Near  
712 Real-time Monitoring and Characterization of Landsat Surface Change for the Conterminous US  
713 (140G0119C0008). We would like to thank Billie Turner II for his insightful comments and  
714 suggestions for this manuscript. The content of this document does not necessarily represent the  
715 views or policies of the Department of the Interior, nor does mention of trade names, commercial  
716 products, or organizations imply endorsement by the U.S. Government.

717

## 718 **Reference**

719 Anderson, J.R., Hardy, E.E., Roach, J.T., Witmer, R.E., 1976. A land use and land cover  
720 classification system for use with remote sensor data, Washington, DC: Government Printing  
721 Office (US Geological Survey, Professional Paper 964). <https://doi.org/10.3133/pp964>  
722 Asner, G.P., Knapp, D.E., Balaji, A., Páez-Acosta, G., 2009. Automated mapping of tropical

723        deforestation and forest degradation: CLASlite. *J. Appl. Remote Sens.* 3, 33543.  
724        <https://doi.org/https://doi.org/10.1117/1.3223675>

725        Asner, G.P., Knapp, D.E., Broadbent, E.N., Oliveira, P.J.C., Keller, M., Silva, J.N., 2005. Selective  
726        logging in the Brazilian Amazon. *Science* 310, 480–482.  
727        <https://doi.org/10.1126/science.1118051>

728        Banskota, A., Kayastha, N., Falkowski, M.J., Wulder, M.A., Froese, R.E., White, J.C., 2014. Forest  
729        monitoring using Landsat time series data: A review. *Can. J. Remote Sens.* 40, 362–384.  
730        <https://doi.org/https://doi.org/10.1080/07038992.2014.987376>

731        Bartels, S.F., Chen, H.Y.H., Wulder, M.A., White, J.C., 2016. Trends in post-disturbance recovery  
732        rates of Canada’s forests following wildfire and harvest. *For. Ecol. Manage.* 361, 194–207.  
733        <https://doi.org/https://doi.org/10.1016/j.foreco.2015.11.015>

734        Belward, A.S., Skøien, J.O., 2015. Who launched what, when and why; trends in global land-cover  
735        observation capacity from civilian earth observation satellites. *ISPRS J. Photogramm. Remote*  
736        *Sens.* 103, 115–128. <https://doi.org/https://doi.org/10.1016/j.isprsjprs.2014.03.009>

737        Bowman, D.M.J.S., Balch, J., Artaxo, P., Bond, W.J., Cochrane, M.A., D’antonio, C.M., DeFries, R.,  
738        Johnston, F.H., Keeley, J.E., Krawchuk, M.A., 2011. The human dimension of fire regimes on  
739        Earth. *J. Biogeogr.* 38, 2223–2236. <https://doi.org/https://doi.org/10.1111/j.1365->  
740        [2699.2011.02595.x](https://doi.org/https://doi.org/10.1111/j.1365-2699.2011.02595.x)

741        Brown, J.F., Tollerud, H.J., Barber, C.P., Zhou, Q., Dwyer, J.L., Vogelmann, J.E., Loveland, T.R.,  
742        Woodcock, C.E., Stehman, S.V., Zhu, Z., Pengra, B.W., 2020. Lessons learned implementing an  
743        operational continuous United States national land change monitoring capability: The Land  
744        Change Monitoring, Assessment, and Project (LCMAP) approach. *Remote Sens. Environ.* 238,  
745        111356. <https://doi.org/10.1016/j.rse.2019.111356>

746        Buchner, J., Yin, H., Frantz, D., Kuemmerle, T., Askerov, E., Bakuradze, T., Bleyhl, B.,  
747        Elizbarashvili, N., Komarova, A., Lewińska, K.E., 2020. Land-cover change in the Caucasus

748 Mountains since 1987 based on the topographic correction of multi-temporal Landsat  
749 composites. *Remote Sens. Environ.* 248, 111967.  
750 <https://doi.org/https://doi.org/10.1016/j.rse.2020.111967>

751 Cho, M.A., Debba, P., Mutanga, O., Dudeni-Tlhone, N., Magadla, T., Khuluse, S.A., 2012. Potential  
752 utility of the spectral red-edge region of SumbandilaSat imagery for assessing indigenous forest  
753 structure and health. *Int. J. Appl. Earth Obs. Geoinf.* 16, 85–93.  
754 <https://doi.org/https://doi.org/10.1016/j.jag.2011.12.005>

755 Claverie, M., Ju, J., Masek, J.G., Dungan, J.L., Vermote, E.F., Roger, J.C., Skakun, S. V., Justice, C.,  
756 2018. The harmonized Landsat and Sentinel-2 surface reflectance data set. *Remote Sens.*  
757 *Environ.* 219, 145–161. <https://doi.org/10.1016/j.rse.2018.09.002>

758 Clements, F.E., 1916. *Plant succession: An analysis of the development of vegetation.* Carnegie  
759 Institution of Washington.

760 Cohen, W.B., Goward, S.N., 2004. Landsat’s role in ecological applications of remote sensing.  
761 *Bioscience* 54, 535–545. [https://doi.org/https://doi.org/10.1641/0006-](https://doi.org/https://doi.org/10.1641/0006-3568(2004)054[0535:LRIEAO]2.0.CO;2)  
762 [3568\(2004\)054\[0535:LRIEAO\]2.0.CO;2](https://doi.org/https://doi.org/10.1641/0006-3568(2004)054[0535:LRIEAO]2.0.CO;2)

763 Coppin, P., Jonckheere, I., Nackaerts, K., Muys, B., Lambin, E., 2004. Digital change detection  
764 methods in ecosystem monitoring: A review. *Int. J. Remote Sens.* 25, 1565–1596.  
765 <https://doi.org/10.1080/0143116031000101675>

766 Coppin, P.R., Bauer, M.E., 1996. Digital change detection in forest ecosystems with remote sensing  
767 imagery. *Remote Sens. Rev.* 13, 207–234.  
768 <https://doi.org/https://doi.org/10.1080/02757259609532305>

769 Dale, V.H., 1997. The relationship between land-use change and climate change. *Ecol. Appl.* 7, 753–  
770 769. [https://doi.org/https://doi.org/10.1890/1051-0761\(1997\)007\[0753:TRBLUC\]2.0.CO;2](https://doi.org/https://doi.org/10.1890/1051-0761(1997)007[0753:TRBLUC]2.0.CO;2)

771 Dale, V.H., Joyce, L.A., McNulty, S., Neilson, R.P., Ayres, M.P., Flannigan, M.D., Hanson, P.J.,  
772 Irland, L.C., Lugo, A.E., Peterson, C.J., 2001. Climate change and forest disturbances: climate

773 change can affect forests by altering the frequency, intensity, duration, and timing of fire,  
774 drought, introduced species, insect and pathogen outbreaks, hurricanes, windstorms, ice storms,  
775 or landslides. *Bioscience* 51, 723–734. [https://doi.org/https://doi.org/10.1641/0006-](https://doi.org/https://doi.org/10.1641/0006-3568(2001)051[0723:CCAFD]2.0.CO;2)  
776 [3568\(2001\)051\[0723:CCAFD\]2.0.CO;2](https://doi.org/https://doi.org/10.1641/0006-3568(2001)051[0723:CCAFD]2.0.CO;2)

777 de Beurs, K.M., Henebry, G.M., Owsley, B.C., Sokolik, I., 2015. Using multiple remote sensing  
778 perspectives to identify and attribute land surface dynamics in Central Asia 2001–2013. *Remote*  
779 *Sens. Environ.* 170, 48–61. <https://doi.org/https://doi.org/10.1016/j.rse.2015.08.018>

780 De Jong, R., Verbesselt, J., Schaepman, M.E., De Bruin, S., 2012. Trend changes in global greening  
781 and browning: Contribution of short-term trends to longer-term change. *Glob. Chang. Biol.* 18,  
782 642–655. <https://doi.org/https://doi.org/10.1111/j.1365-2486.2011.02578.x>

783 Deng, C., Zhu, Z., 2020. Continuous subpixel monitoring of urban impervious surface using Landsat  
784 time series. *Remote Sens. Environ.* 238, 110929. <https://doi.org/10.1016/j.rse.2018.10.011>

785 Drusch, M., Del Bello, U., Carlier, S., Colin, O., Fernandez, V., Gascon, F., Hoersch, B., Isola, C.,  
786 Laberinti, P., Martimort, P., Meygret, A., Spoto, F., Sy, O., Marchese, F., Bargellini, P., 2012.  
787 Sentinel-2: ESA’s Optical High-Resolution Mission for GMES Operational Services. *Remote*  
788 *Sens. Environ.* 120, 25–36. <https://doi.org/10.1016/j.rse.2011.11.026>

789 Dwyer, J., Roy, D., Sauer, B., Jenkerson, C., Zhang, H., Lymburner, L., 2018. Analysis Ready Data:  
790 Enabling Analysis of the Landsat Archive. *Remote Sens.* 10, 1363.  
791 <https://doi.org/10.3390/rs10091363>

792 Eidenshink, J., Schwind, B., Brewer, K., Zhu, Z., Quayle, B., Howard, S., Falls, S., Falls, S., 2007. A  
793 Project for Monitoring Trends in Burn Severity. *Fire Ecol.* 3, 3–21.  
794 <https://doi.org/10.4996/fireecology.0301003>

795 Eitel, J., Vierling, L.A., Litvak, M.E., Long, D.S., Schulthess, U., Ager, A., Dan, J.K., Stoscheck, L.,  
796 2011. Broadband, red-edge information from satellites improves early stress detection in a New  
797 Mexico conifer woodland. *Remote Sens. Environ.* 115, 3640–3646.

798 <https://doi.org/https://doi.org/10.1016/j.rse.2011.09.002>

799 Ellis, E.C., Klein Goldewijk, K., Siebert, S., Lightman, D., Ramankutty, N., 2010. Anthropogenic  
800 transformation of the biomes, 1700 to 2000. *Glob. Ecol. Biogeogr.* 19, 589–606.  
801 <https://doi.org/https://doi.org/10.1111/j.1466-8238.2010.00540.x>

802 Elvidge, C.D., Zhizhin, M., Ghosh, T., Hsu, F.-C., Taneja, J., 2021. Annual time series of global  
803 VIIRS nighttime lights derived from monthly averages: 2012 to 2019. *Remote Sens.*  
804 <https://doi.org/10.3390/rs13050922>

805 Foody, G.M., Doan, H.T.X., 2007. Variability in soft classification prediction and its implications for  
806 sub-pixel scale change detection and super resolution mapping. *Photogramm. Eng. Remote*  
807 *Sens.* 73, 923–933. <https://doi.org/https://doi.org/10.14358/PERS.73.8.923>

808 Frantz, D., 2019. FORCE—Landsat+ Sentinel-2 analysis ready data and beyond. *Remote Sens.* 11,  
809 1124. <https://doi.org/https://doi.org/10.3390/rs11091124>

810 Frantz, D., Haß, E., Uhl, A., Stoffels, J., Hill, J., 2018. Improvement of the Fmask algorithm for  
811 Sentinel-2 images: Separating clouds from bright surfaces based on parallax effects. *Remote*  
812 *Sens. Environ.* 215, 471–481. <https://doi.org/10.1016/j.rse.2018.04.046>

813 Friis, C., Nielsen, J.Ø., Otero, I., Haberl, H., Niewöhner, J., Hostert, P., 2016. From teleconnection to  
814 telecoupling: Taking stock of an emerging framework in land system science. *J. Land Use Sci.*  
815 11, 131–153. <https://doi.org/https://doi.org/10.1080/1747423X.2015.1096423>

816 Gao, F., Masek, J.G., Wolfe, R.E., 2009. Automated registration and orthorectification package for  
817 Landsat and Landsat-like data processing. *J. Appl. Remote Sens.* 3, 033515.  
818 <https://doi.org/10.1117/1.3104620>

819 Garbulsky, M.F., Peñuelas, J., Gamon, J., Inoue, Y., Filella, I., 2011. The photochemical reflectance  
820 index (PRI) and the remote sensing of leaf, canopy and ecosystem radiation use efficiencies: A  
821 review and meta-analysis. *Remote Sens. Environ.* 115, 281–297.  
822 <https://doi.org/https://doi.org/10.1016/j.rse.2010.08.023>

823 Geist, H.J., Lambin, E.F., 2002. Proximate Causes and Underlying Driving Forces of Tropical  
824 Deforestation Tropical forests are disappearing as the result of many pressures, both local and  
825 regional, acting in various combinations in different geographical locations. *Bioscience* 52, 143–  
826 150. [https://doi.org/https://doi.org/10.1641/0006-3568\(2002\)052\[0143:PCAUDF\]2.0.CO;2](https://doi.org/10.1641/0006-3568(2002)052[0143:PCAUDF]2.0.CO;2)

827 Giglio, L., Boschetti, L., Roy, D.P., Humber, M.L., Justice, C.O., 2018. The Collection 6 MODIS  
828 burned area mapping algorithm and product. *Remote Sens. Environ.* 217, 72–85.  
829 [https://doi.org/https://doi.org/10.1016/j.rse.2018.08.005](https://doi.org/10.1016/j.rse.2018.08.005)

830 Gómez, C., White, J.C., Wulder, M.A., 2016. Optical remotely sensed time series data for land cover  
831 classification: A review. *ISPRS J. Photogramm. Remote Sens.* 116, 55–72.  
832 <https://doi.org/10.1016/j.isprsjprs.2016.03.008>

833 Gorelick, N., Hancher, M., Dixon, M., Ilyushchenko, S., Thau, D., Moore, R., 2017. Google Earth  
834 Engine: Planetary-scale geospatial analysis for everyone. *Remote Sens. Environ.* 202, 18–27.  
835 [https://doi.org/https://doi.org/10.1016/j.rse.2017.06.031](https://doi.org/10.1016/j.rse.2017.06.031)

836 Grime, J.P., 1977. Evidence for the existence of three primary strategies in plants and its relevance to  
837 ecological and evolutionary theory. *Am. Nat.* 111, 1169–1194.

838 Guo, X., Feng, J., Shi, Z., Zhou, X., Yuan, M., Tao, X., Hale, L., Yuan, T., Wang, J., Qin, Y., 2018.  
839 Climate warming leads to divergent succession of grassland microbial communities. *Nat. Clim.*  
840 *Chang.* 8, 813–818. [https://doi.org/https://doi.org/10.1038/s41558-018-0254-2](https://doi.org/10.1038/s41558-018-0254-2)

841 Gutman, G., Janetos, A.C., Justice, C.O., Moran, E.F., Mustard, J.F., Rindfuss, R.R., Skole, D.,  
842 Turner II, B.L., Cochrane, M.A., 2004. Land change science: observing, monitoring and  
843 understanding trajectories of change on the earth’s surface. Springer Science & Business Media.

844 Hansen, M.C., DeFries, R.S., 2004. Detecting long-term global forest change using continuous fields  
845 of tree-cover maps from 8-km advanced very high resolution radiometer (AVHRR) data for the  
846 years 1982–99. *Ecosystems* 7, 695–716. [https://doi.org/http://dx.doi.org/10.1007%2Fs10021-](https://doi.org/http://dx.doi.org/10.1007%2Fs10021-004-0243-3)  
847 [004-0243-3](https://doi.org/http://dx.doi.org/10.1007%2Fs10021-004-0243-3)

848 Hansen, M.C., Loveland, T.R., 2012. A review of large area monitoring of land cover change using  
849 Landsat data. *Remote Sens. Environ.* 122, 66–74. <https://doi.org/10.1016/j.rse.2011.08.024>

850 Hansen, M.C., Potapov, P.V., Moore, R., Hancher, M., Turubanova, S.A.A., Tyukavina, A., Thau,  
851 D., Stehman, S.V., Goetz, S.J., Loveland, T.R., Kommareddy, A., 2013. High-resolution global  
852 maps of 21st-century forest cover change. *Science* 342, 850–853.  
853 <https://doi.org/10.1126/science.1244693>

854 Healey, S.P., Cohen, W.B., Yang, Z., Kenneth Brewer, C., Brooks, E.B., Gorelick, N., Hernandez,  
855 A.J., Huang, C., Joseph Hughes, M., Kennedy, R.E., Loveland, T.R., Moisen, G.G., Schroeder,  
856 T.A., Stehman, S. V., Vogelmann, J.E., Woodcock, C.E., Yang, L., Zhu, Z., 2018. Mapping  
857 forest change using stacked generalization: An ensemble approach. *Remote Sens. Environ.* 204,  
858 717–728. <https://doi.org/10.1016/j.rse.2017.09.029>

859 Huang, C., Goward, S.N., Masek, J.G., Thomas, N., Zhu, Z., Vogelmann, J.E., 2010. An automated  
860 approach for reconstructing recent forest disturbance history using dense Landsat time series  
861 stacks. *Remote Sens. Environ.* 114, 183–198. <https://doi.org/10.1016/j.rse.2009.08.017>

862 Huang, H., Roy, D.P., 2021. Characterization of Planetscope-0 Planetscope-1 surface reflectance and  
863 normalized difference vegetation index continuity. *Sci. Remote Sens.* 3, 100014.  
864 <https://doi.org/https://doi.org/10.1016/j.srs.2021.100014>

865 Huang, X., Cao, Y., Li, J., 2020. An automatic change detection method for monitoring newly  
866 constructed building areas using time-series multi-view high-resolution optical satellite images.  
867 *Remote Sens. Environ.* 244, 111802. <https://doi.org/https://doi.org/10.1016/j.rse.2020.111802>

868 Huete, A., 2016. Vegetation’s responses to climate variability. *Nature* 531, 181–182.  
869 <https://doi.org/https://doi.org/10.1038/nature17301>

870 Huston, M., Smith, T., 1987. Plant succession: life history and competition. *Am. Nat.* 130, 168–198.  
871 <https://doi.org/https://doi.org/10.1016/j.ecoleng.2021.106331>

872 Jensen, J.R., 2009. *Remote sensing of the environment: An earth resource perspective 2/e*. Pearson

873 Education India.

874 Jiao, Z., Woodcock, C., Schaaf, C.B., Tan, B., Liu, J., Gao, F., Strahler, A., Li, X., Wang, J., 2011.

875 Improving MODIS land cover classification by combining MODIS spectral and angular

876 signatures in a Canadian boreal forest. *Can. J. Remote Sens.* 37, 184–203.

877 <https://doi.org/10.5589/m11-030>

878 Jin, S., Homer, C., Yang, L., Danielson, P., Dewitz, J., Li, C., Zhu, Z., Xian, G., Howard, D., 2019.

879 Overall methodology design for the United States national land cover database 2016 products.

880 *Remote Sens.* 11. <https://doi.org/10.3390/rs11242971>

881 Jin, S., Sader, S.A., 2005. MODIS time-series imagery for forest disturbance detection and

882 quantification of patch size effects. *Remote Sens. Environ.* 99, 462–470.

883 <https://doi.org/10.1016/j.rse.2005.09.017>

884 Johnson, E.A., Miyanishi, K., 2021. Disturbance and succession, in: Johnson, E.A., Miyanishi,

885 K.B.T.-P.D.E. (Second E. (Eds.), *Plant Disturbance Ecology*. Academic Press, San Diego, pp.

886 1–15. <https://doi.org/https://doi.org/10.1016/B978-0-12-818813-2.00001-0>

887 Johnson, E.W., Wittwer, D., 2008. Aerial detection surveys in the United States. *Aust. For.* 71, 212–

888 215. <https://doi.org/10.1080/00049158.2008.10675037>

889 Justice, C.O., Giglio, L., Korontzi, S., Owens, J., Morisette, J.T., Roy, D., Descloitres, J., Alleaume,

890 S., Petitcolin, F., Kaufman, Y., 2002. The MODIS fire products. *Remote Sens. Environ.* 83,

891 244–262. [https://doi.org/https://doi.org/10.1016/S0034-4257\(02\)00076-7](https://doi.org/https://doi.org/10.1016/S0034-4257(02)00076-7)

892 Justice, C.O., Vermote, E., Townshend, J.R.G., Defries, R., Roy, D.P., Hall, D.K., Salomonson, V.

893 V., Privette, J.L., Riggs, G., Strahler, A., 1998. The Moderate Resolution Imaging

894 Spectroradiometer (MODIS): Land remote sensing for global change research. *IEEE Trans.*

895 *Geosci. Remote Sens.* 36, 1228–1249.

896 Kennedy, R.E., Andréfouët, S., Cohen, W.B., Gómez, C., Griffiths, P., Hais, M., Healey, S.P.,

897 Helmer, E.H., Hostert, P., Lyons, M.B., 2014. Bringing an ecological view of change to

898 Landsat-based remote sensing. *Front. Ecol. Environ.* 12, 339–346.  
899 <https://doi.org/https://doi.org/10.1890/130066>

900 Kennedy, R.E., Cohen, W.B., Schroeder, T.A., 2007. Trajectory-based change detection for  
901 automated characterization of forest disturbance dynamics. *Remote Sens. Environ.* 110, 370–  
902 386. <https://doi.org/https://doi.org/10.1016/j.rse.2007.03.010>

903 Kennedy, R.E., Yang, Z., Braaten, J., Copass, C., Antonova, N., Jordan, C., Nelson, P., 2015.  
904 Attribution of disturbance change agent from Landsat time-series in support of habitat  
905 monitoring in the Puget Sound region, USA. *Remote Sens. Environ.* 166, 271–285.  
906 <https://doi.org/10.1016/j.rse.2015.05.005>

907 Kirschbaum, D.B., Adler, R., Hong, Y., Hill, S., Lerner-Lam, A., 2010. A global landslide catalog for  
908 hazard applications: method, results, and limitations. *Nat. Hazards* 52, 561–575.  
909 <https://doi.org/10.1007/s11069-009-9401-4>

910 Knoflach, B., Ramskogler, K., Talluto, M., Hofmeister, F., Haas, F., Heckmann, T., Pfeiffer, M.,  
911 Piermattei, L., Ressler, C., Wimmer, M.H., 2021. Modelling of Vegetation Dynamics from  
912 Satellite Time Series to Determine Proglacial Primary Succession in the Course of Global  
913 Warming—A Case Study in the Upper Martell Valley (Eastern Italian Alps). *Remote Sens.* 13,  
914 4450.

915 Laflour, D.M., Hurteau, M.D., Koch, G.W., North, M.P., Hungate, B.A., 2016. Climate-driven  
916 changes in forest succession and the influence of management on forest carbon dynamics in the  
917 Puget Lowlands of Washington State, USA. *For. Ecol. Manage.* 362, 194–204.  
918 <https://doi.org/https://doi.org/10.1016/j.foreco.2015.12.015>

919 Lambin, E.F., Strahlers, A.H., 1994. Change-vector analysis in multitemporal space: A tool to detect  
920 and categorize land-cover change processes using high temporal-resolution satellite data.  
921 *Remote Sens. Environ.* 48, 231–244. [https://doi.org/https://doi.org/10.1016/0034-](https://doi.org/https://doi.org/10.1016/0034-4257(94)90144-9)  
922 [4257\(94\)90144-9](https://doi.org/https://doi.org/10.1016/0034-4257(94)90144-9)

923 Lambin, E.F., Turner, B.L., Geist, H.J., Agbola, S.B., Angelsen, A., Bruce, J.W., Coomes, O.T.,  
924 Dirzo, R., Fischer, G., Folke, C., 2001. The causes of land-use and land-cover change: Moving  
925 beyond the myths. *Glob. Environ. Chang.* 11, 261–269.  
926 [https://doi.org/https://doi.org/10.1016/S0959-3780\(01\)00007-3](https://doi.org/https://doi.org/10.1016/S0959-3780(01)00007-3)

927 Lawrence, R., 2005. Remote sensing of vegetation responses during the first 20 years following the  
928 1980 eruption of Mount St. Helens: a spatially and temporally stratified analysis, in: *Ecological*  
929 *Responses to the 1980 Eruption of Mount St. Helens*. Springer, New York, NY, pp. 111–123.  
930 [https://doi.org/https://doi.org/10.1007/0-387-28150-9\\_8](https://doi.org/https://doi.org/10.1007/0-387-28150-9_8)

931 Lentile, L.B., Holden, Z.A., Smith, A.M.S., Falkowski, M.J., Hudak, A.T., Morgan, P., Lewis, S.A.,  
932 Gessler, P.E., Benson, N.C., 2006. Remote sensing techniques to assess active fire  
933 characteristics and post-fire effects. *Int. J. Wildl. Fire* 15, 319–345.  
934 <https://doi.org/https://doi.org/10.1071/WF05097>

935 Levin, Noam, 2017. The impact of seasonal changes on observed nighttime brightness from 2014 to  
936 2015 monthly VIIRS DNB composites. *Remote Sens. Environ.* 193, 150–164.  
937 <https://doi.org/https://doi.org/10.1016/j.rse.2017.03.003>

938 Li, J., Roy, D.P., 2017. A global analysis of Sentinel-2A, Sentinel-2B and Landsat-8 data revisit  
939 intervals and implications for terrestrial monitoring. *Remote Sens.* 9, 902.  
940 <https://doi.org/10.3390/rs9090902>

941 Lin, Y., Zhu, Z., Guo, W., Sun, Y., Yang, X., Kovalskyy, V., 2020. Continuous monitoring of cotton  
942 stem water potential using Sentinel-2 imagery. *Remote Sens.* 12, 1176.  
943 <https://doi.org/https://doi.org/10.3390/rs12071176>

944 Liu, H., Gong, P., Wang, J., Wang, X., Ning, G., Xu, B., 2021. Production of global daily seamless  
945 data cubes and quantification of global land cover change from 1985 to 2020 - iMap World 1.0.  
946 *Remote Sens. Environ.* 258, 112364. <https://doi.org/10.1016/j.rse.2021.112364>

947 Liu, X., Huang, Y., Xu, X., Li, Xuecao, Li, Xia, Ciais, P., Lin, P., Gong, K., Ziegler, A.D., Chen, A.,

948 Gong, P., Chen, J., Hu, G., Chen, Y., Wang, S., Wu, Q., Huang, K., Estes, L., Zeng, Z., 2020.  
949 High-spatiotemporal-resolution mapping of global urban change from 1985 to 2015. *Nat.*  
950 *Sustain.* 3, 564–570. <https://doi.org/10.1038/s41893-020-0521-x>

951 Liu, Y., Wang, Z., Sun, Q., Erb, A.M., Li, Z., Schaaf, C.B., Zhang, X., Román, M.O., Scott, R.L.,  
952 Zhang, Q., Novick, K.A., Sydonia Bret-Harte, M., Petroy, S., SanClements, M., 2017.  
953 Evaluation of the VIIRS BRDF, Albedo and NBAR products suite and an assessment of  
954 continuity with the long term MODIS record. *Remote Sens. Environ.* 201, 256–274.  
955 <https://doi.org/https://doi.org/10.1016/j.rse.2017.09.020>

956 Liu, Y., Xu, B., Zhi, W., Hu, C., Dong, Y., Jin, S., Lu, Y., Chen, T., Xu, W., Liu, Yongchao, Zhao,  
957 B., Lu, W., 2020. Space eye on flying aircraft: From Sentinel-2 MSI parallax to hybrid  
958 computing. *Remote Sens. Environ.* 246, 111867.  
959 <https://doi.org/https://doi.org/10.1016/j.rse.2020.111867>

960 Loveland, T.R., Sohl, T.L., Stehman, S. V, Gallant, A.L., Sayler, K.L., Napton, D.E., 2002. A  
961 strategy for estimating the rates of recent United States land-cover changes. *Photogramm. Eng.*  
962 *Remote Sensing* 68, 1091–1099.

963 Ma, Y., Wu, H., Wang, L., Huang, B., Ranjan, R., Zomaya, A., Jie, W., 2015. Remote sensing big  
964 data computing: Challenges and opportunities. *Futur. Gener. Comput. Syst.* 51, 47–60.  
965 <https://doi.org/10.1016/j.future.2014.10.029>

966 Martin, L., Howarth, P.J., 1989. Change-detection accuracy assessment using SPOT multispectral  
967 imagery of the rural-urban fringe. *Remote Sens. Environ.* 30, 55–66.  
968 [https://doi.org/10.1016/0034-4257\(89\)90047-3](https://doi.org/10.1016/0034-4257(89)90047-3)

969 Masek, J.G., Vermote, E.F., Saleous, N.E., Wolfe, R., Hall, F.G., Huemmrich, K.F., Gao, F., Kutler,  
970 J., Lim, T.-K., 2006. A Landsat surface reflectance dataset for North America, 1990-2000. *IEEE*  
971 *Geosci. Remote Sens. Lett.* 3, 68–72. <https://doi.org/10.1109/LGRS.2005.857030>

972 Masek, J.G., Wulder, M.A., Markham, B., McCorkel, J., Crawford, C.J., Storey, J., Jenstrom, D.T.,

973 2020. Landsat 9: Empowering open science and applications through continuity. *Remote Sens.*  
974 *Environ.* 248, 111968. <https://doi.org/10.1016/j.rse.2020.111968>

975 Mildrexler, D.J., Zhao, M., Running, S.W., 2009. Testing a MODIS global disturbance index across  
976 North America. *Remote Sens. Environ.* 113, 2103–2117.  
977 <https://doi.org/https://doi.org/10.1016/j.rse.2009.05.016>

978 Myneni, R.B., Keeling, C.D., Tucker, C.J., Asrar, G., Nemani, R.R., 1997. Increased plant growth in  
979 the northern high latitudes from 1981 to 1991. *Nature* 386, 698–702.  
980 <https://doi.org/10.1038/386698a0>

981 NOAA, 2022. Severe Weather Data Inventory [WWW Document]. NOAA. URL  
982 <https://www.ncei.noaa.gov/products/severe-weather-data-inventory> (accessed 1.4.22).

983 NRC, 1999. Human dimensions of global environmental change: Research pathways for the next  
984 decade. National Academies Press.

985 NRC, 1998. People and pixels: Linking remote sensing and social science. National Academies  
986 Press.

987 Oeser, J., Pflugmacher, D., Senf, C., Heurich, M., Hostert, P., 2017. Using intra-annual Landsat time  
988 series for attributing forest disturbance agents in Central Europe. *Forests* 8, 251.  
989 <https://doi.org/https://doi.org/10.3390/f8070251>

990 Olofsson, P., Foody, G.M., Stehman, S. V, Woodcock, C.E., 2013. Making better use of accuracy  
991 data in land change studies: Estimating accuracy and area and quantifying uncertainty using  
992 stratified estimation. *Remote Sens. Environ.* 129, 122–131.  
993 <https://doi.org/https://doi.org/10.1016/j.rse.2012.10.031>

994 Pekel, J.-F., Cottam, A., Gorelick, N., Belward, A.S., 2016. High-resolution mapping of global  
995 surface water and its long-term changes. *Nature* 540, 418–422.  
996 <https://doi.org/10.1038/nature20584>

997 Pengra, B.W., Stehman, S. V., Horton, J.A., Dockter, D.J., Schroeder, T.A., Yang, Z., Cohen, W.B.,

998 Healey, S.P., Loveland, T.R., 2020. Quality control and assessment of interpreter consistency of  
999 annual land cover reference data in an operational national monitoring program. *Remote Sens.*  
1000 *Environ.* 238, 111261. <https://doi.org/10.1016/j.rse.2019.111261>

1001 Pesaresi, M., Ehrlich, D., Ferri, S., Florczyk, A., Freire, S., Halkia, M., Julea, A., Kemper, T., Soille,  
1002 P., Syrris, V., 2016. Operating procedure for the production of the Global Human Settlement  
1003 Layer from Landsat data of the epochs 1975, 1990, 2000, and 2014, Luxembourg  
1004 (Luxembourg): Publications Office of the European Union. <https://doi.org/10.2788/656115>

1005 Peters, D.P.C., Lugo, A.E., Chapin III, F.S., Pickett, S.T.A., Duniway, M., Rocha, A. V, Swanson,  
1006 F.J., Laney, C., Jones, J., 2011. Cross-system comparisons elucidate disturbance complexities  
1007 and generalities. *Ecosphere* 2, 1–26. <https://doi.org/https://doi.org/10.1890/ES11-00115.1>

1008 Petit, C., Scudder, T., Lambin, E., 2001. Quantifying processes of land-cover change by remote  
1009 sensing: resettlement and rapid land-cover changes in south-eastern Zambia. *Int. J. Remote*  
1010 *Sens.* 22, 3435–3456. <https://doi.org/https://doi.org/10.1080/01431160010006881>

1011 Potter, C., TAN, P., Steinbach, M., Klooster, S., Kumar, V., Myneni, R., Genovese, V., 2003. Major  
1012 disturbance events in terrestrial ecosystems detected using global satellite data sets. *Glob.*  
1013 *Chang. Biol.* 9, 1005–1021. <https://doi.org/10.1046/j.1365-2486.2003.00648.x>

1014 Pricope, N.G., Mapes, K.L., Woodward, K.D., 2019. Remote Sensing of Human–Environment  
1015 Interactions in Global Change Research: A Review of Advances, Challenges and Future  
1016 Directions. *Remote Sens.* <https://doi.org/10.3390/rs11232783>

1017 Qin, Y., Xiao, X., Wigneron, J.-P., Ciais, P., Brandt, M., Fan, L., Li, X., Crowell, S., Wu, X.,  
1018 Doughty, R., 2021. Carbon loss from forest degradation exceeds that from deforestation in the  
1019 Brazilian Amazon. *Nat. Clim. Chang.* 11, 442–448.  
1020 <https://doi.org/https://doi.org/10.1038/s41558-021-01026-5>

1021 Qiu, S., Lin, Y., Shang, R., Zhang, J., Ma, L., Zhu, Z., Qiu, S., Lin, Y., Shang, R., Zhang, J., Ma, L.,  
1022 Zhu, Z., 2019a. Making Landsat Time Series Consistent: Evaluating and Improving Landsat

1023 Analysis Ready Data. *Remote Sens.* 11. <https://doi.org/10.3390/RS11010051>

1024 Qiu, S., Zhu, Z., He, B., 2019b. Fmask 4.0: Improved cloud and cloud shadow detection in Landsats  
1025 4–8 and Sentinel-2 imagery. *Remote Sens. Environ.* 231, 111205.  
1026 <https://doi.org/10.1016/j.rse.2019.05.024>

1027 Riemann, R., Wilson, B.T., Lister, A., Parks, S., 2010. An effective assessment protocol for  
1028 continuous geospatial datasets of forest characteristics using USFS Forest Inventory and  
1029 Analysis (FIA) data. *Remote Sens. Environ.* 114, 2337–2352.  
1030 <https://doi.org/https://doi.org/10.1016/j.rse.2010.05.010>

1031 Rindfuss, R.R., Walsh, S.J., Turner, B.L., Fox, J., Mishra, V., 2004. Developing a science of land  
1032 change: challenges and methodological issues. *Proc. Natl. Acad. Sci.* 101, 13976–13981.  
1033 <https://doi.org/https://doi.org/10.1073/pnas.0401545101>

1034 Rollins, M.G., 2009. LANDFIRE: A nationally consistent vegetation, wildland fire, and fuel  
1035 assessment. *Int. J. Wildl. Fire* 18, 235–249. <https://doi.org/10.1071/WF08088>

1036 Román, M.O., Wang, Z., Sun, Q., Kalb, V., Miller, S.D., Molthan, A., Schultz, L., Bell, J., Stokes,  
1037 E.C., Pandey, B., 2018. NASA’s Black Marble nighttime lights product suite. *Remote Sens.*  
1038 *Environ.* 210, 113–143. <https://doi.org/https://doi.org/10.1016/j.rse.2018.03.017>

1039 Roy, D.P., Huang, H., Houborg, R., Martins, V.S., 2021. A global analysis of the temporal  
1040 availability of PlanetScope high spatial resolution multi-spectral imagery. *Remote Sens.*  
1041 *Environ.* 264, 112586. <https://doi.org/https://doi.org/10.1016/j.rse.2021.112586>

1042 Roy, D.P., Wulder, M.A., Loveland, T.R., C.E., W., Allen, R.G., Anderson, M.C., Helder, D., Irons,  
1043 J.R., Johnson, D.M., Kennedy, R., Scambos, T.A., Schaaf, C.B., Schott, J.R., Sheng, Y.,  
1044 Vermote, E.F., Belward, A.S., Bindschadler, R., Cohen, W.B., Gao, F., Hipple, J.D., Hostert, P.,  
1045 Huntington, J., Justice, C.O., Kilic, A., Kovalsky, V., Lee, Z.P., Lyburner, L., Masek, J.G.,  
1046 McCorkel, J., Shuai, Y., Trezza, R., Vogelmann, J., Wynne, R.H., Zhu, Z., 2014. Landsat-8:  
1047 Science and product vision for terrestrial global change research. *Remote Sens. Environ.* 145,

1048 154–172. <https://doi.org/10.1016/j.rse.2014.02.001>

1049 Roy, D.P., Zhang, H.K., Ju, J., Gomez-Dans, J.L., Lewis, P.E., Schaaf, C.B., Sun, Q., Li, J., Huang,  
1050 H., Kovalskyy, V., 2016. A general method to normalize Landsat reflectance data to nadir  
1051 BRDF adjusted reflectance. *Remote Sens. Environ.* 176, 255–271.  
1052 <https://doi.org/10.1016/j.rse.2016.01.023>

1053 Saleska, S.R., Didan, K., Huete, A.R., Da Rocha, H.R., 2007. Amazon forests green-up during 2005  
1054 drought. *Science* 318, 612. <https://doi.org/10.1126/science.1146663>

1055 Samanta, A., Ganguly, S., Hashimoto, H., Devadiga, S., Vermote, E., Knyazikhin, Y., Nemani, R.R.,  
1056 Myneni, R.B., 2010. Amazon forests did not green-up during the 2005 drought. *Geophys. Res.*  
1057 *Lett.* 37. <https://doi.org/https://doi.org/10.1029/2009GL042154>

1058 Schaaf, C.B., Gao, F., Strahler, A.H., Lucht, W., Li, X., Tsang, T., Strugnell, N.C., Zhang, X., Jin,  
1059 Y., Muller, J.-P.P., Lewis, P., Barnsley, M., Hobson, P., Disney, M., Roberts, G., Dunderdale,  
1060 M., Doll, C., D'Entremont, R.P., Hu, B., Liang, S., Privette, J.L., Roy, D., 2002. First  
1061 operational BRDF, albedo nadir reflectance products from MODIS. *Remote Sens. Environ.* 83,  
1062 135–148. [https://doi.org/10.1016/S0034-4257\(02\)00091-3](https://doi.org/10.1016/S0034-4257(02)00091-3)

1063 Schroeder, T.A., Schleeweis, K.G., Moisen, G.G., Toney, C., Cohen, W.B., Freeman, E.A., Yang, Z.,  
1064 Huang, C., 2017. Testing a Landsat-based approach for mapping disturbance causality in U.S.  
1065 forests. *Remote Sens. Environ.* 195, 230–243. <https://doi.org/10.1016/j.rse.2017.03.033>

1066 Sebal, J., Senf, C., Seidl, R., 2021. Human or natural? Landscape context improves the attribution  
1067 of forest disturbances mapped from Landsat in Central Europe. *Remote Sens. Environ.* 262,  
1068 112502. <https://doi.org/https://doi.org/10.1016/j.rse.2021.112502>

1069 Seidl, R., Thom, D., Kautz, M., Martin-Benito, D., Peltoniemi, M., Vacchiano, G., Wild, J., Ascoli,  
1070 D., Petr, M., Honkaniemi, J., 2017. Forest disturbances under climate change. *Nat. Clim. Chang.*  
1071 7, 395–402. <https://doi.org/https://doi.org/10.1038/nclimate3303>

1072 Sellers, P.J., Meeson, B.W., Hall, F.G., Asrar, G., Murphy, R.E., Schiffer, R.A., Bretherton, F.P.,

1073 Dickinson, R.E., Ellingson, R.G., Field, C.B., 1995. Remote sensing of the land surface for  
1074 studies of global change: Models—algorithms—experiments. *Remote Sens. Environ.* 51, 3–26.  
1075 [https://doi.org/https://doi.org/10.1016/0034-4257\(94\)00061-Q](https://doi.org/https://doi.org/10.1016/0034-4257(94)00061-Q)

1076 Senf, C., Seidl, R., Hostert, P., 2017. Remote sensing of forest insect disturbances: Current state and  
1077 future directions. *Int. J. Appl. Earth Obs. Geoinf.* 60, 49–60.  
1078 <https://doi.org/https://doi.org/10.1016/j.jag.2017.04.004>

1079 Seto, K.C., Reenberg, A., Boone, C.G., Fragkias, M., Haase, D., Langanke, T., Marcotullio, P.,  
1080 Munroe, D.K., Olah, B., Simon, D., 2012. Urban land teleconnections and sustainability. *Proc.*  
1081 *Natl. Acad. Sci.* 109, 7687–7692. <https://doi.org/https://doi.org/10.1073/pnas.1117622109>

1082 Shang, R., Zhu, Z., 2019. Harmonizing Landsat 8 and Sentinel-2: A time-series-based reflectance  
1083 adjustment approach. *Remote Sens. Environ.* 235, 111439.  
1084 <https://doi.org/10.1016/j.rse.2019.111439>

1085 Shimizu, K., Ota, T., Mizoue, N., Yoshida, S., 2019. A comprehensive evaluation of disturbance  
1086 agent classification approaches: Strengths of ensemble classification, multiple indices, spatio-  
1087 temporal variables, and direct prediction. *ISPRS J. Photogramm. Remote Sens.* 158, 99–112.  
1088 <https://doi.org/https://doi.org/10.1016/j.isprsjprs.2019.10.004>

1089 Sohl, T.L., Gallant, A.L., Loveland, T.R., 2004. The characteristics and interpretability of land  
1090 surface change and implications for project design. *Photogramm. Eng. Remote Sensing* 70, 439–  
1091 448. <https://doi.org/10.14358/PERS.70.4.439>

1092 Song, C., Woodcock, C.E., Seto, K.C., Lenney, M.P., Macomber, S.A., 2001. Classification and  
1093 change detection using Landsat TM data: When and how to correct atmospheric effects? *Remote*  
1094 *Sens. Environ.* 75, 230–244. [https://doi.org/10.1016/S0034-4257\(00\)00169-3](https://doi.org/10.1016/S0034-4257(00)00169-3)

1095 Song, X.P., Hansen, M.C., Stehman, S. V., Potapov, P. V., Tyukavina, A., Vermote, E.F.,  
1096 Townshend, J.R., 2018. Global land change from 1982 to 2016. *Nature* 560, 639–643.  
1097 <https://doi.org/10.1038/s41586-018-0411-9>

1098 Sousa, W.P., 1984. The role of disturbance in natural communities. *Annu. Rev. Ecol. Syst.* 15, 353–  
1099 391.

1100 Szostak, M., Hawryło, P., Piela, D., 2018. Using of Sentinel-2 images for automation of the forest  
1101 succession detection. *Eur. J. Remote Sens.* 51, 142–149.  
1102 <https://doi.org/10.1080/22797254.2017.1412272>

1103 Tan, B., Masek, J.G., Wolfe, R., Gao, F., Huang, C., Vermote, E.F., Sexton, J.O., Ederer, G., 2013.  
1104 Improved forest change detection with terrain illumination corrected Landsat images. *Remote  
1105 Sens. Environ.* 136, 469–483. <https://doi.org/https://doi.org/10.1016/j.rse.2013.05.013>

1106 Tang, X., Bullock, E.L., Olofsson, P., Estel, S., Woodcock, C.E., 2019. Near real-time monitoring of  
1107 tropical forest disturbance: New algorithms and assessment framework. *Remote Sens. Environ.*  
1108 224, 202–218. <https://doi.org/https://doi.org/10.1016/j.rse.2019.02.003>

1109 Tellman, B., Magliocca, N.R., Turner, B.L., Verburg, P.H., 2020. Understanding the role of illicit  
1110 transactions in land-change dynamics. *Nat. Sustain.* 3, 175–181. [https://doi.org/10.1038/s41893-  
1111 019-0457-1](https://doi.org/10.1038/s41893-019-0457-1)

1112 Tollerud, H.J., Brown, J.F., Loveland, T.R., 2020. Investigating the effects of land use and land cover  
1113 on the relationship between moisture and reflectance using Landsat time series. *Remote Sens.*  
1114 12, 1919. <https://doi.org/https://doi.org/10.3390/rs12121919>

1115 Turner, B.L., 1997. The sustainability principle in global agendas: implications for understanding  
1116 land-use/cover change. *Geogr. J.* 163, 133–140.

1117 Turner, B.L., Lambin, E.F., Reenberg, A., 2007. The emergence of land change science for global  
1118 environmental change and sustainability. *Proc. Natl. Acad. Sci.* 104, 20666–20671.  
1119 <https://doi.org/https://doi.org/10.1073/pnas.0704119104>

1120 Turner, B.L., Lambin, E.F., Verburg, P.H., 2021. From land-use/land-cover to land system science.  
1121 *Ambio* 50, 1291–1294. <https://doi.org/10.1007/s13280-021-01510-4>

1122 Turner, M.G., 2010. Disturbance and landscape dynamics in a changing world. *Ecology* 91, 2833–

1123 2849. <https://doi.org/https://doi.org/10.1890/10-0097.1>

1124 Ustin, S.L., Middleton, E.M., 2021. Current and near-term advances in Earth observation for  
1125 ecological applications. *Ecol. Process.* 10, 1–57. [https://doi.org/https://doi.org/10.1186/s13717-](https://doi.org/https://doi.org/10.1186/s13717-020-00255-4)  
1126 020-00255-4

1127 Verbesselt, J., Hyndman, R., Newnham, G., Culvenor, D., 2010. Detecting trend and seasonal  
1128 changes in satellite image time series. *Remote Sens. Environ.* 114, 106–115.  
1129 <https://doi.org/10.1016/j.rse.2009.08.014>

1130 Verbesselt, J., Zeileis, A., Herold, M., 2012. Near real-time disturbance detection using satellite  
1131 image time series. *Remote Sens. Environ.* 123, 98–108.  
1132 <https://doi.org/https://doi.org/10.1016/j.rse.2012.02.022>

1133 Verrelst, J., Camps-Valls, G., Muñoz-Marí, J., Rivera, J.P., Veroustraete, F., Clevers, J.G.P.W.,  
1134 Moreno, J., 2015. Optical remote sensing and the retrieval of terrestrial vegetation bio-  
1135 geophysical properties—A review. *ISPRS J. Photogramm. Remote Sens.* 108, 273–290.  
1136 <https://doi.org/https://doi.org/10.1016/j.isprsjprs.2015.05.005>

1137 Verstraete, M.M., Pinty, B., 1996. Designing optimal spectral indexes for remote sensing  
1138 applications. *IEEE Trans. Geosci. Remote Sens.* 34, 1254–1265.

1139 Vogelmann, J.E., Gallant, A.L., Shi, H., Zhu, Z., 2016. Perspectives on monitoring gradual change  
1140 across the continuity of Landsat sensors using time-series data. *Remote Sens. Environ.* 185,  
1141 258–270. <https://doi.org/10.1016/j.rse.2016.02.060>

1142 Vogelmann, J.E., Xian, G., Homer, C., Tolk, B., 2012. Monitoring gradual ecosystem change using  
1143 Landsat time series analyses: Case studies in selected forest and rangeland ecosystems. *Remote*  
1144 *Sens. Environ.* 122, 92–105. <https://doi.org/https://doi.org/10.1016/j.rse.2011.06.027>

1145 Wang, Z., Román, M.O., Kalb, V.L., Miller, S.D., Zhang, J., Shrestha, R.M., 2021. Quantifying  
1146 uncertainties in nighttime light retrievals from Suomi-NPP and NOAA-20 VIIRS Day/Night  
1147 Band data. *Remote Sens. Environ.* 263, 112557.

1148 <https://doi.org/https://doi.org/10.1016/j.rse.2021.112557>

1149 White, P.S., Pickett, S.T.A., 1985. Natural disturbance and patch dynamics: an introduction, in:

1150 PICKETT, S.T.A., WHITE, P.S.B.T.-T.E. of N.D. and P.D. (Eds.), *The Ecology of Natural*

1151 *Disturbance and Patch Dynamics*. Academic Press, San Diego, pp. 3–13.

1152 <https://doi.org/https://doi.org/10.1016/B978-0-08-050495-7.50006-5>

1153 Woodcock, C.E., Allen, R., Anderson, M., Belward, A., Bindschadler, R., Cohen, W., Gao, F.,

1154 Goward, S.N., Helder, D., Helmer, E., Nemani, R., Oreopoulos, L., Schott, J., Thenkabail, P.S.,

1155 Vermote, E.F., Vogelmann, J., Wulder, M.A., Wynne, R., 2008. Free access to Landsat imagery.

1156 *Science* 320, 1011–1011. <https://doi.org/10.1126/science.320.5879.1011a>

1157 Woodcock, C.E., Loveland, T.R., Herold, M., Bauer, M.E., 2020. Transitioning from change

1158 detection to monitoring with remote sensing: A paradigm shift. *Remote Sens. Environ.* 238,

1159 111558. <https://doi.org/https://doi.org/10.1016/j.rse.2019.111558>

1160 Woodcock, C.E., Strahler, A.H., 1987. The factor of scale in remote sensing. *Remote Sens. Environ.*

1161 21, 311–332. [https://doi.org/https://doi.org/10.1016/0034-4257\(87\)90015-0](https://doi.org/https://doi.org/10.1016/0034-4257(87)90015-0)

1162 Wulder, M.A., Masek, J.G., Cohen, W.B., Loveland, T.R., Woodcock, C.E., 2012. Opening the

1163 archive: How free data has enabled the science and monitoring promise of Landsat. *Remote*

1164 *Sens. Environ.* 122, 2–10. <https://doi.org/10.1016/j.rse.2012.01.010>

1165 Xin, Q.C., Olofsson, P., Zhu, Z., Tan, B., Woodcock, C.E., 2013. Toward near real-time monitoring

1166 of forest disturbance by fusion of MODIS and Landsat data. *Remote Sens. Environ.* 135, 234–

1167 247. <https://doi.org/10.1016/J.Rse.2013.04.002>

1168 Yan, L., Roy, D.P., Zhang, H., Li, J., Huang, H., 2016. An automated approach for sub-pixel

1169 registration of Landsat-8 Operational Land Imager (OLI) and Sentinel-2 Multi Spectral

1170 Instrument (MSI) imagery. *Remote Sens.* 8, 520.

1171 <https://doi.org/https://doi.org/10.3390/rs8060520>

1172 Ye, S., Rogan, J., Zhu, Z., Eastman, J.R., 2021a. A near-real-time approach for monitoring forest

1173 disturbance using Landsat time series: Stochastic continuous change detection. *Remote Sens.*  
1174 *Environ.* 252, 112167. <https://doi.org/https://doi.org/10.1016/j.rse.2020.112167>

1175 Ye, S., Rogan, J., Zhu, Z., Hawbaker, T.J., Hart, S.J., Andrus, R.A., Meddens, A.J.H., Hicke, J.A.,  
1176 Eastman, J.R., Kulakowski, D., 2021b. Detecting subtle change from dense Landsat time series:  
1177 Case studies of mountain pine beetle and spruce beetle disturbance. *Remote Sens. Environ.* 263,  
1178 112560. <https://doi.org/https://doi.org/10.1016/j.rse.2021.112560>

1179 Zhang, J., Shang, R., Rittenhouse, C., Witharana, C., Zhu, Z., 2021. Evaluating the impacts of  
1180 models, data density and irregularity on reconstructing and forecasting dense Landsat time  
1181 series. *Sci. Remote Sens.* 100023. <https://doi.org/https://doi.org/10.1016/j.srs.2021.100023>

1182 Zhao, F., Huang, C., Goward, S.N., Schleeweis, K., Rishmawi, K., Lindsey, M.A., Denning, E.,  
1183 Keddell, L., Cohen, W.B., Yang, Z., Dungan, J.L., Michaelis, A., 2018. Development of  
1184 Landsat-based annual US forest disturbance history maps (1986–2010) in support of the North  
1185 American Carbon Program (NACP). *Remote Sens. Environ.* 209, 312–326.  
1186 <https://doi.org/https://doi.org/10.1016/j.rse.2018.02.035>

1187 Zhao, F.R., Meng, R., Huang, C., Zhao, M., Zhao, F.A., Gong, P., Yu, L., Zhu, Z., 2016. Long-term  
1188 post-disturbance forest recovery in the greater Yellowstone ecosystem analyzed using Landsat  
1189 time series stack. *Remote Sens.* 8, 898. <https://doi.org/https://doi.org/10.3390/rs8110898>

1190 Zhu, Z., 2019. Science of Landsat analysis ready data. *Remote Sens.* 11, 2166.  
1191 <https://doi.org/https://doi.org/10.3390/rs11182166>

1192 Zhu, Z., 2017. Change detection using landsat time series: A review of frequencies, preprocessing,  
1193 algorithms, and applications. *ISPRS J. Photogramm. Remote Sens.* 130, 370–384.  
1194 <https://doi.org/10.1016/j.isprsjprs.2017.06.013>

1195 Zhu, Zhe, Fu, Y., Woodcock, C.E., Olofsson, P., Vogelmann, J.E., Holden, C., Wang, M., Dai, S.,  
1196 Yu, Y., 2016. Including land cover change in analysis of greenness trends using all available  
1197 Landsat 5, 7, and 8 images: A case study from Guangzhou, China (2000–2014). *Remote Sens.*

1198 Environ. 185, 243–257. <https://doi.org/10.1016/j.rse.2016.03.036>

1199 Zhu, Zaichun, Piao, S., Myneni, R.B., Huang, M., Zeng, Z., Canadell, J.G., Ciais, P., Sitch, S.,  
1200 Friedlingstein, P., Arneth, A., Cao, C., Cheng, L., Kato, E., Koven, C., Li, Y., Lian, X., Liu, Y.,  
1201 Liu, R., Mao, J., Pan, Y., Peng, S., Peuelas, J., Poulter, B., Pugh, T.A.M., Stocker, B.D., Viovy,  
1202 N., Wang, X., Wang, Y., Xiao, Z., Yang, H., Zaehle, S., Zeng, N., 2016. Greening of the Earth  
1203 and its drivers. *Nat. Clim. Chang.* 6, 791–795. <https://doi.org/10.1038/nclimate3004>

1204 Zhu, Z., Qiu, S., He, B., Deng, C., 2018. Cloud and cloud shadow detection for Landsat images : the  
1205 fundamental basis for analyzing Landsat time series. *Remote Sens. Time Ser. Image Process.* 3–  
1206 24. <https://doi.org/10.1201/9781315166636-10>

1207 Zhu, Z., Woodcock, C.E., 2014. Continuous change detection and classification of land cover using  
1208 all available Landsat data. *Remote Sens. Environ.* 144, 152–171.  
1209 <https://doi.org/10.1016/j.rse.2014.01.011>

1210 Zhu, Z., Woodcock, C.E., 2012. Object-based cloud and cloud shadow detection in Landsat imagery.  
1211 *Remote Sens. Environ.* 118, 83–94. <https://doi.org/10.1016/j.rse.2011.10.028>

1212 Zhu, Z., Woodcock, C.E., Olofsson, P., 2012. Continuous monitoring of forest disturbance using all  
1213 available Landsat imagery. *Remote Sens. Environ.* 122, 75–91.  
1214 <https://doi.org/10.1016/j.rse.2011.10.030>

1215 Zhu, Z., Wulder, M.A., Roy, D.P., Woodcock, C.E., Hansen, M.C., Radeloff, V.C., Healey, S.P.,  
1216 Schaaf, C., Hostert, P., Strobl, P., Pekel, J.F., Lyburner, L., Pahlevan, N., Scambos, T.A.,  
1217 2019. Benefits of the free and open Landsat data policy. *Remote Sens. Environ.* 224, 382–385.  
1218 <https://doi.org/10.1016/j.rse.2019.02.016>

1219 Zhu, Z., Zhang, J., Yang, Z., Aljaddani, A.H., Cohen, W.B., Qiu, S., Zhou, C., 2020. Continuous  
1220 monitoring of land disturbance based on Landsat time series. *Remote Sens. Environ.* 238,  
1221 111116. <https://doi.org/10.1016/j.rse.2019.03.009>

1222

